The Thesis Committee for Colin James Capello
Certifies that this is the approved version of the following thesis:

Fluid retention in textured surfaces under shear flow conditions

APPROVED BY
SUPERVISING COMMITTEE:

Supervisor:

Vaibhav Bahadur

Yaguo Wang

Fluid retention in textured surfaces under shear flow conditions

by

Colin James Capello, B.S.

Thesis

Presented to the Faculty of the Graduate School of

The University of Texas at Austin

in Partial Fulfillment

of the Requirements

for the Degree of

Master of Science in Engineering

The University of Texas at Austin

August 2016

Dedicated to my loving wife for her continual support

Acknowledgements

First and foremost I would like to thank my advisor Dr. Bahadur for his guidance and support throughout this research. I also would like to thank my lab mates Renee Hale, Katie Carpenter, Mark Hermes, and Enakshi Wikramanayake who provided insight and encouragement along the way. I would like to thank Dr. Wang for agreeing to be my second reader. Lastly, I would like to thank my wife and family for their support along the way that made all of this possible.

Abstract

Fluid retention in textured surfaces under shear flow conditions

Colin James Capello, M.S.E.

The University of Texas at Austin, 2016

Supervisor: Vaibhav Bahadur

The ability of a surface to retain water or oil has oil-gas flow assurance applications like hydrocarbon deposition prevention, oil-water separation and core annular flows. This dissertation examines the ability of textured aluminum surfaces to retain water or oil. The surface texture is obtained by an acid treatment of aluminum; the high surface energy and the porous texture (resulting from the chemical etching) together creates a surface which can wick liquid into its interior. Strong adhesion between the surface and liquid is expected to lead to a stable film, even in the presence of liquid shear.

This dissertation presents preliminary experimental results that are the first step towards understanding the ability of textured surfaces in retaining liquid under shear flow conditions. A custom built recirculating flow loop is used to measure the ability of the surface to retain oil and water under the action of water and oil shear flow respectively. It is seen that the surface can retain oil films under water flows as high as 0.26 m/s (Reynolds number of 9900). The surface showed loss of water films under an oil flow velocity of 0.13 m/s (Reynolds number of 500); additional experiments are needed to

determine the utility of such surfaces in retaining water at lower speeds. Similarly, oil loss from the surface was observed under the action of water jet impingement.

Additionally, this work examined the chemical resistance of the textured aluminum surface by exposure to five liquid media. It was observed that static tap water does not degrade the performance of the surface, which validates the use of such surfaces in a wide variety of operating conditions. High temperature water exposure can degrade surface performance due to bubbling-induced fluid loss from the textures. The surfaces show performance degradation under concentrated acidic and basic media exposure; however, they are expected to offer more resistance in lower concentrations that approach real world conditions.

Overall, this work provides preliminary assessments and a starting point for an understanding of the interfacial phenomena involved in liquid retention on textured surfaces. Follow-up studies will ultimately enable the development of surface architectures for trapping fluids for various oil-gas applications.

Table of Contents

List of Tables

List of Figures

Chapter 1

Introduction

This dissertation analyzes a recently developed technology concept for oil-gas flow assurance applications, such as hydrocarbon fouling mitigation, heavy oil pumping via core annular flows, and oil-water separation. By keeping a surface water wetted in the presence of hydrocarbon flow, hydrocarbon-surface contact can be minimized, which will reduce the chances of fouling and deposition of organic entities such as asphaltenes, waxes and hydrates. Furthermore, the pumping power to transport heavy viscous oil can be drastically reduced by lubricating oil flow with a thin water layer; this technology is known as core-annular flow (Figure 1).

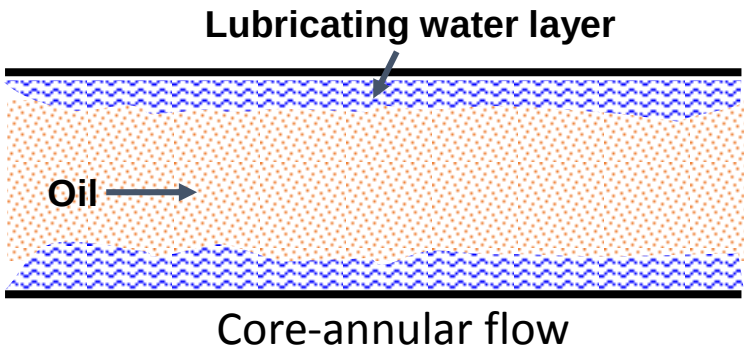

Figure 1. Illustration of core-annular flows with the oil flow lubricated by a thin layer of water.

Maintaining a stable water film at the surface can be a challenge due to the shearing action of oil flow. Coatings which are hydrophilic in an oil environment can significantly aid the retention of this water film. One such coating, recently developed in the current research group, is analyzed in the present work. This coating is made by etching pure aluminum in an acid solution; the chemical reaction leads to a porous texture on the surface, which is extremely hydrophilic in an air environment. This surface

absorbs and retains water (or oil), that is brought into contact with it. The stability of this water (or oil) layer under the action of liquid shear is unknown. The work presented in this dissertation quantifies the retention of a liquid film on the etched aluminum surface under the action of shear flow. This dissertation also analyzes the robustness and durability of the etched aluminum surfaces.

It is noted that this dissertation is a follow-up to previous work [2] in the group on the use of electrowetting for maintaining a thin water film on the surface in a hydrocarbon medium. Electrowetting (EW) is the increase in wettability of conducting liquids via the application of an interfacial electric field [1]. EW can be exploited to keep a surface water-wet and displace non-conducting liquids away from the surface. Previous work reported measurements of the electrically tunable water droplet-surface adhesion. Adhesion was measured in terms of the tilt angle needed to roll off an electrowetted droplet from the surface. Measurements showed a 67% increase in droplet-surface adhesion at a 20 V/μm electric field [2].

This dissertation does not analyze the use of electric fields for maintaining a stable water film. Instead the approach is to use extremely hydrophilic (in an oil environment) coatings to maintain this water film. Such an approach would avoid the costs and complexities associated with introducing electrical systems in the oil-gas production and transport processes.

It should also be noted that the concept of water-wetting a surface has been studied by other researchers [3, 4]. The concept of core annular flows (for heavy oil transport) has been studied by other researchers [5, 6, 7, 8, 9]. However, one of the biggest challenges in implementing this technology is the instability of the water film and issues related to stratification after shutdown. The proposed work presents an alternative strategy to keep surfaces water-wet in an oil flow environment.

Another aspect of flow assurance that can be impacted by the present work is the area of oil-water separation. Oil production is always accompanied by water production, and separating water from oil can be challenging. Plate separators can be used to enhance gravity aided separation. Separation technology can benefit from the development of both water-loving (in oil) surfaces and oil-loving (in water) surfaces. The present work therefore also examines the stability of oil films in a water environment, in addition to the stability of water films in an oil environment.

1.1. INTRODUCTION TO DROPLET-SURFACE ADHESION

The primary focus of this thesis is to determine the durability of an etched aluminum surface and quantify its ability to retain liquid in its porous matrix. The adhesion between the surface and a droplet on the surface can be used to quantify the effectiveness of the surface in retaining liquid. In this dissertation, the adhesion is primarily quantified in terms of the wettability of the surface. It is important to note that wettability is not the only method for quantifying liquid-surface adhesion.

Adhesion of a droplet to a surface depends upon surface roughness and the chemistry of the surface and the liquid [10, 11, 12, 13]. Young's equation can be used to determine the equilibrium contact angles of a droplet on a given surface. Young's equation predicts the contact angles in terms of interfacial energies as:

$$\cos(\theta_Y) = \frac{\sigma_{sv} - \sigma_{sl}}{\sigma_{lv}} \quad (1)$$

where θ_Y is Young's contact angle, σ_{sv} is the solid-vapor interfacial energy, σ_{sl} is the solid-liquid interfacial energy and σ_{lv} is the liquid-vapor interfacial energy [13, 14]. Through the contact angle, Young's equation provides a first order understanding of

wettability, which can be used to quantify surface adhesion. Higher contact angles indicate a hydrophobic surface (in air) with lower adhesion, while lower contact angles indicate a hydrophilic surface (in air) with higher adhesion [13]. When surface roughness is negligible, i.e. a smooth surface, the contact angle depends solely on the interfacial energies. When a surface is not smooth, surface roughness related effects must also be considered [13].

Two extreme and contrasting cases are traditionally used to understand the effects of surface roughness on contact angles. These cases are the Cassie and Wenzel state, which illustrate how drops can interact with a rough and textured surface [11, 12]. Figure 2 shows the surface-droplet contact in both states. In the Cassie state, the droplet rests on the tips of the roughness causing elements of a surface. This state has a small liquid-surface contact area, which indicates low droplet-surface adhesion and a low friction. A good example of the Cassie state is seen with water droplets on the Teflon coated etched aluminum samples in Figure A3 in the appendix. The Wenzel state is more applicable to a majority of the droplet-surface interactions presented in this dissertation. In the Wenzel state, a droplet completely wets the rough surface. This results in large liquid-surface contact area and high adhesion. The present work seeks to exploit the high adhesion of the Wenzel state to maintain a stable water film at the surface in the presence of oil shear.

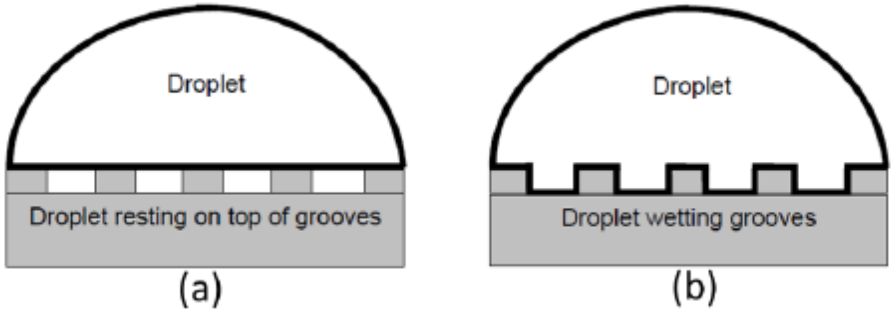

Figure 2. Droplets on rough surfaces (a) Cassie-Baxter State (b) Wenzel State [15].

1.2. OUTLINE OF DISSERTATION

Chapter 2 presents experimental studies to ascertain the durability and performance degradation of etched aluminum surfaces. The first set of experiments analyze the chemical resistance of the etched aluminum surfaces by measuring the effectiveness of such surfaces in retaining an oil film after the surfaces have been exposed to various chemical media.

Chapter 3 presents the results of experimental studies to study the stability of water (and oil films) under shear. Such flow experiments were conducted in a custom built flow loop that could achieve fluid speeds of 9.6 m/s. Chapter 3 also presents results of another experimental study in which a high pressure water stream was used to remove oil from the textured aluminum surfaces. Overall, the experiments in Chapter 3 quantify the ability of the surfaces to retain liquid in the presence of shear forces. Chapter 4 summarizes the findings of this dissertation and includes suggestions for future work. An appendix is included that contains additional tables and figures.

Chapter 2

Durability and chemical resistance of etched aluminum surfaces

This chapter details studies to measure the durability and chemical resistance of the etched aluminum surfaces. Firstly, the procedure to measure adhesion (wettability) of these surfaces is detailed. Subsequently, the method of fabrication of the etched aluminum surfaces is described. This is followed by wettability measurements on these surfaces. The following section details the experiments used to measure surface durability, where etched aluminum surfaces were left immersed in various fluids to determine performance degradation.

2.1. WETTABILITY MEASUREMENTS

Adhesion measurements were made using One Attension's Theta optical tensiometer, or goniometer (Figure 3), by measuring the contact angle of water droplets. The Theta goniometer has a three axis adjustable platform that samples can be placed upon for measurements. A camera is used by the goniometer to measure contact angles, and can be moved along rails to adjust its location relative to the sample. The focus of the camera and zoom of the lens can also be adjusted. The instrument interfaces with a computer using One Attension's proprietary software, OneAttension, to allow the user to measure various parameters of the droplet and droplet-surface adhesion. The first order Young-Laplace equation was used in these experiments to determine the contact angle of the droplets.

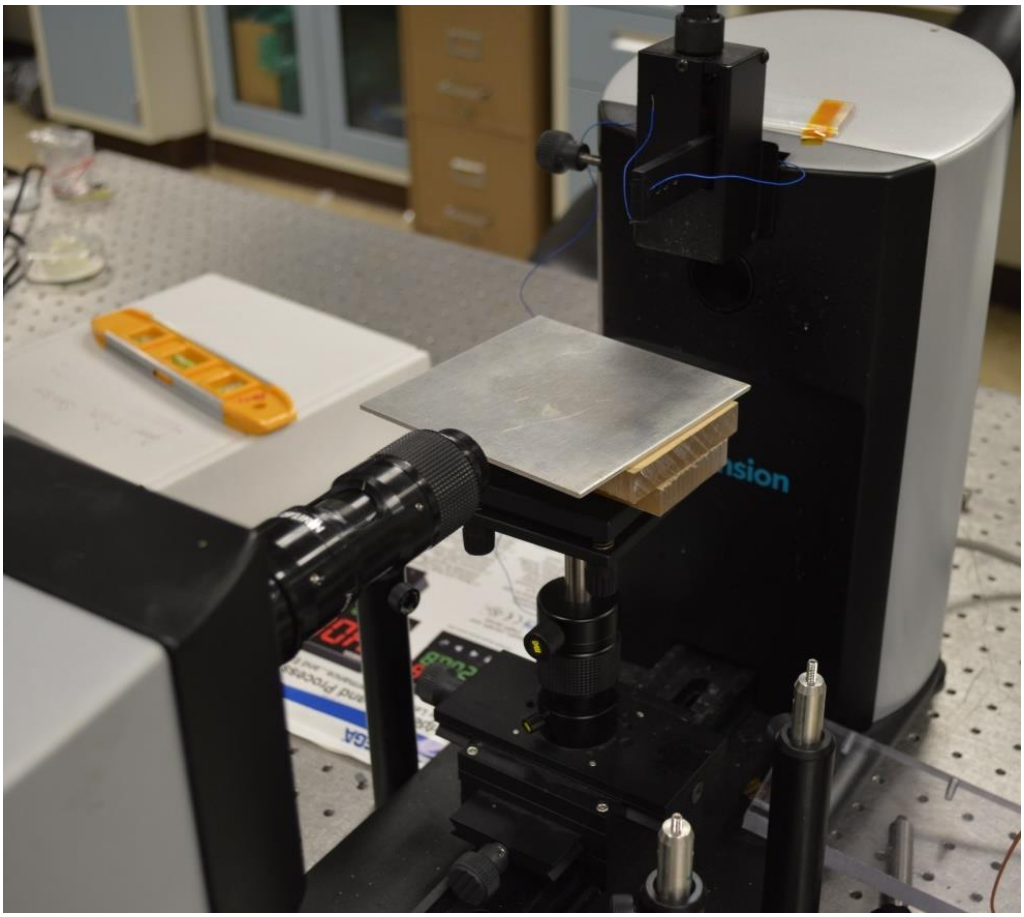

Figure 3. OneAttension Theta Goniometer.

2.2. FABRICATION OF ETCHED ALUMINUM SURFACES

In this section the procedure for fabricating the etched aluminum surfaces is detailed. When pure aluminum is immersed in hydrochloric acid for an extended period of time, the acid reacts with aluminum to form aluminum chloride. In this process, the surface is converted to a porous textured surface with high surface energy [16]. Such surfaces are expected to be hydrophilic; indeed the surface acts as a wick when exposed to liquids such as oil and water. The surface will absorb the first liquid exposed to and will retain the liquid within its pores.

The substrates used in these experiments were polished aluminum wafers, cut to 2 inches by 1 inch using a reciprocating saw. The sample was then cleaned with acetone or isopropyl alcohol and allowed to air dry. The sample was then placed in a container with a lid and immersed in a bath of 3 molar hydrochloric acid for at least fifteen minutes. To ensure uniform etching there are two conditions that should be met related to the level of the hydrochloric acid and the etch time. The level of the hydrochloric acid should be at least 2 mm above the top of the sample to ensure that the top of the sample is fully etched. The samples should be immersed for enough time to allow for complete etching of the surface. Thicker samples will require more than fifteen minutes of immersion time to ensure that the surface is completely etched.

Post etch, the sample was rinsed with deionized water and soaked in a bath of DI water at 100° C for an hour. During both the etching and soaking phase it is imperative that the samples do not rest on top of each other, or else the etching on the surface may be non-uniform. Upon completion of the water soaking step, the samples were rinsed in DI water and placed on a hot plate at 120° C to dry the samples. Visually, the surfaces appeared uniform, and absorbed water and oil into its porous surface layer. SEM (Scanning electron microscope) images of the etched aluminum surfaces can be seen in Figures 4-7. Figures 4-6 show the etched aluminum surface with increasing magnification, while Figure 7 shows the surface at a 20° tilt. It is clearly seen, that the etched layer is textured and porous; these pores can trap and retain liquid. The SEM images were taken by Enakshi Wikramanayake (a PhD student) in the research group.

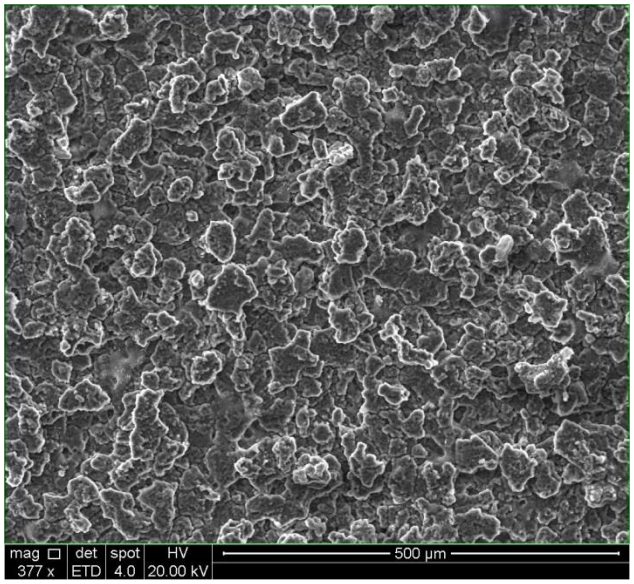

Figure 4. SEM image of etched aluminum at a magnification of 377.

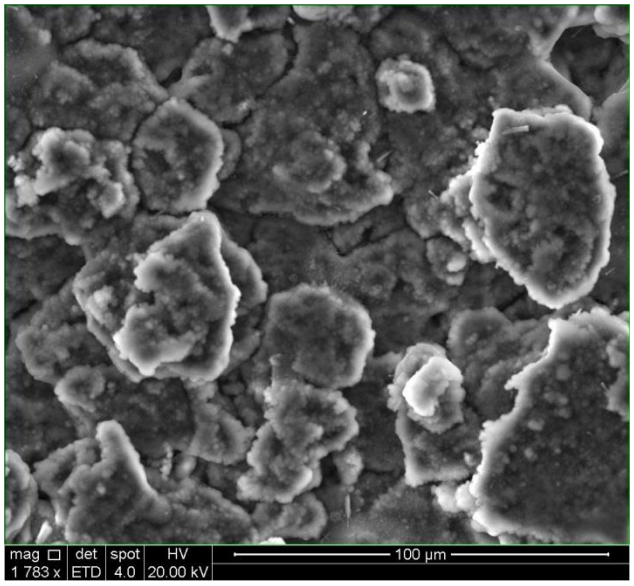

Figure 5. SEM image of etched aluminum at a magnification of 1783.

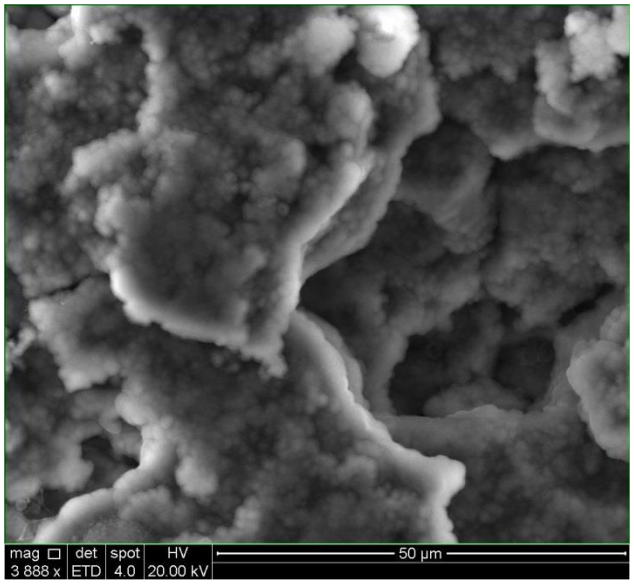

Figure 6. SEM image of etched aluminum at a magnification of 3888.

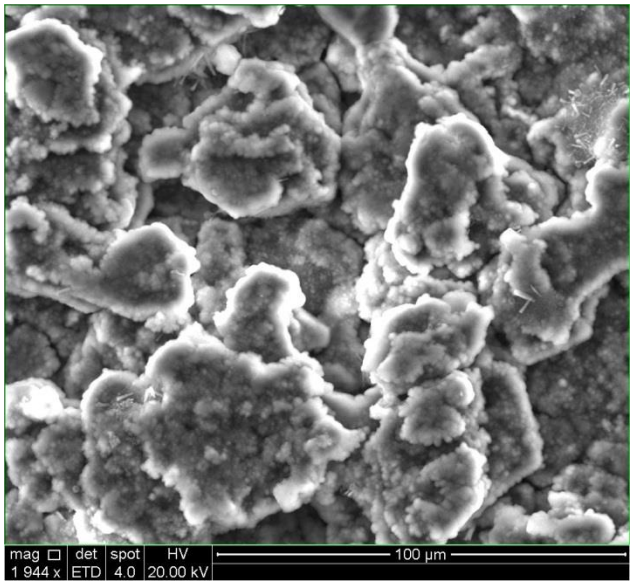

Figure 7. SEM image of etched aluminum (sample tilted by 20°) at a magnification of 1944.

Some surfaces were spin coated with Teflon after they were dry. The Teflon coated textured samples are intended to be used in future studies of oil-water separation, since only oil can wet the textures (and not water). Teflon AF 1600 was spin coated at

2000 rpm for a minute, followed by a bake at 245° C for twenty minutes. This resulted in an approximate Teflon thickness of 125 nanometers.

2.3. PRELIMINARY MEASUREMENTS OF WETTABILITY

Contact angles of water droplets on polished aluminum were measured to establish a procedure for future contact angle measurements and to establish a baseline. 10 microliter droplets were deposited on the polished aluminum samples; a minimum of five drops was used per sample on various locations along the surface. The goniometer allows a series of photos to be taken in quick succession to create a video that can be analyzed. A ten second video at 20 frames per second was recorded for each trial allowing for 200 contact angle measurements to be reported per droplet. The goniometer sets an automatic baseline for analyzing the contact angle, else one can be set manually. The program then reports contact angles on both sides of the droplet as well as the average . The contact angles for the polished aluminum samples ranged from 76° to 79°. The contact angles of the Teflon coated etched aluminum samples ranged from 155° to 160°. This procedure for measuring contact angles is used for all the work reported in the dissertation.

2.4. MEASURING CHEMICAL RESISTANCE AND PERFORMANCE DEGRADATION OF ETCHED ALUMINUM SURFACES

Robustness and chemical resistance of the etched aluminum surfaces is an important parameter to ascertain the viability of such surfaces for practical applications. This section details the experimental procedure utilized to characterize the chemical resistance and robustness of such surfaces. Chemical resistance was determined by

exposing the surface to various chemical solutions. Since many solutions were water-based, it was decided to measure the oil retention ability of such surfaces, after exposure to the chemical solutions. Olive oil (density~ 910 kg/m^3, viscosity~ 91.5 cSt at 22° C) was the oil selected for these experiments [17, 18]. The performance degradation of the surface was measured by qualitative observations of the surface post chemical exposure and contact angle measurements.

Five liquids were used in these experiments: tap water at room temperature (22° C), boiling tap water (100° C), 0.6 molar hydrochloric acid, 0.6 molar sodium hydroxide, and acetone. These liquids represent a range of fouling and corrosion causing environments.

The hardware used for these experiments included the One Attension goniometer to measure contact angles, sealable glass containers for immersing the samples, a spin coater to fabricate the Teflon coated samples, and a hot plate to maintain the boiling water bath.

The procedure for these experiments can be summarized as follows. The surface was first fabricated and infused with oil. The excess oil was allowed to roll off the surface and the baseline contact angle of water was measured. The surfaces were then immersed in the test liquid solution for a pre-decided time, following which the contact angle was again measured.

The etched aluminum surfaces (with and without Teflon coatings) were immersed in an olive oil bath for a minimum of four hours to ensure that the oil fully absorbs into the surface. The Teflon samples took two to three times as long as the uncoated samples to absorb the oil. Once the oil infusion was completed, the samples were removed from the bath and leaned on a side face to allow excess oil to drain off of the surface. The excess oil was gravity drained. It was determined that sufficient oil has been removed

when there was no visibly pooled oil when the sample was laid flat; Figure A4 in the appendix shows an example of this. It was found that wiping or using compressed air removes the oil unevenly, which can affect contact angle measurements. Using a wipe could also deposit foreign particles on the surface, and the compressed air could possibly remove oil absorbed inside the texture of the surface. Following oil removal, the contact angles of water droplets were measured using the process described earlier. The samples were then placed in a liquid bath and allowed to soak in the chemical medium for the desired amount of time. At the completion of the soak time the samples were dried in the same manner as after removal from the oil bath, and the contact angle measurements were repeated. Each experiment was conducted with a minimum of two samples per fluid. Care was taken to keep the surfaces in the same orientation throughout the whole experiment, as the side of the surface facing up will be etched to a greater extent.

2.5. RESULTS - CHEMICAL RESISTANCE OF SURFACES IN VARIOUS LIQUID MEDIA

This section summarizes the results of the experiments with the five liquids. Qualitative observations of performance degradation of the surfaces are described. Quantitative data showing the contact angle variation versus immersion time is also presented.

2.5.1. Immersion liquid - Room temperature tap water

The first fluid explored in this work was tap water at room temperature (22° C). The objective was to ascertain, whether exposure to water would remove the oil, based on the density difference between the two fluids. The samples were submerged for a total of 24 hours, while contact angles were recorded after 15 minutes, 60 minutes, and 24 hours.

After the tap water soak, the water rolled off the surface, which was a visual cue that the oil was present within the textures of the etched aluminum surface. The contact angle of the water droplet on the oil infused surface versus time can be seen in Table 1. Overall, there is no significant change in contact angle from the tap water soak even after 24 hours. This leads to the conclusion that the density difference does not provide enough of a driving force to remove the oil trapped in the texture of the etched aluminum surface. Pictures of the samples after the test are included in the appendix (Figure A8).

Table 1. Contact angle of water droplets on an oil-infused etched aluminum surface versus time after exposure to room temperature tap water.

Time (min)	Sample 1	Sample 2	Average
0	74.0	72.7	73.3
15	76.8	67.1	71.9
60	79.4	66.7	73.0
1440	82.4	82.3	82.4

2.5.2. Immersion liquid - Boiling tap water

The next set of experiments explored the effects of boiling water on the oil-infused surface. Initially a glass beaker was used for these experiments. However, due to the insulating nature of glass, and large convective losses, the water could not reach boiling conditions in an efficient manner. Subsequently, a stainless steel pan with a lid was used for these experiments. The water bath's lid was not closed, as there were safety concerns from a potential release of built up high pressure steam. This led to the need for periodic refilling of the water bath with tap water after approximately 4 hours. The

samples were immersed in boiling water for 24 hours. The contact angle data for these tests is shown in Table 2 and Table 3, for etched aluminum and Teflon coated etched aluminum surfaces respectively.

The results indicate that boiling water removed oil from the pores of the etched aluminum surface (Table 2). After 24 hours, water droplets were being wicked into the surface, which indicates the absence of oil in the texture. Bubble nucleation and growth-forced oil expulsion from the texture is a likely mechanism to explain oil removal. This trend was observed for all of the samples except for Sample 35, which exhibited hydrophobicity after 24 hours. Sample 35 appeared visually different than the other five samples at the 24 hour mark and it was placed in the boiling water bath for an additional 12 hours. Pictures of Sample 35 can be seen in the appendix (Figure A9). After the additional soaking time, Sample 35 exhibited the same characteristics as the other three etched samples. This leads to the conclusion boiling water can remove the olive oil from the etched aluminum surface's textures.

Table 2. Contact angle of water droplets on an oil-infused etched aluminum surface versus time after exposure to boiling tap water.

Time (hour)	Sample 31	Sample 32	Sample 35	Sample 36	Average
0	78.2	80.8	77	76.8	78.2
24	0	0	123	0	30.8
36	-	-	0	-	0
168, no water	0	0	0	0	0

Boiling water was able to remove oil from the texture even for the Teflon coated etched aluminum surfaces (Table 3). At the 24 hour mark, the contact angle measurements also yielded 0°. The boiling water removed the olive oil and also appeared to breakdown the Teflon layer.

Table 3. Contact angle of water droplets on an oil-infused etched aluminum surface (Teflon coated) versus time after exposure to boiling tap water.

Time (hour)	Sample 33	Sample 34	Sample 37	Sample 38	Average
0	76	76.4	79.3	78.8	77.6
24	0	0	0	0	0
24, no water	-	-	0	0	0
168, no water	0	0	-	-	0

After these measurements, the samples were placed on a hot plate again to remove any residual water in the surface's matrix. The samples were then left exposed to air for either a 24 hour period or a 7 day period. The surfaces absorbed water into the structure, in a manner consistent to oil not being present. One thought was that oil might be still trapped deep in the surface's matrix and would migrate to the surface with time; however, this was not observed. The contact angle was 0° for all of these tests. Pictures of the samples after the tests can be seen in the appendix (Figure A10).

Overall, these experiments are significant, since they show that exposure to boiling water can remove oil from the pores, and render the surfaces unusable.

2.5.3. Immersion liquid - Hydrochloric acid solution

The chemical resistance of the surfaces to acidic media was characterized by exposing them to a room temperature hydrochloric acid solution. 0.6 molarity hydrochloric acid (HCl) was used for these experiments, which is five times less concentrated than the solution used for etching aluminum. The samples were placed in a closed and sealed container. Contact angles were measured at 15 minutes, 60 minutes, and 24 hours for the etched aluminum samples. For the Teflon coated etched aluminum surfaces, measurements were done at 60 minutes and 24 hours. The experimental data for etched aluminum and Teflon coated etched aluminum surfaces are shown in Tables 4 and 5 respectively.

From the results for etched aluminum surfaces (Table 4), it appears that the porous, textured layer is removed upon exposure to acid solutions, which releases the trapped oil. The contact angle drops to 0° because the surface now infuses the water droplet used for the contact angle measurements. For the Teflon coated samples (Table 5), the oil layer is again removed and the Teflon layer appears to be breaking down, which can be seen in pictures in the appendix (Figure A12). Contact angles for the etched aluminum and the Teflon coated etched aluminum surfaces are close to the values for water droplets in the absence of oil.

Table 4. Contact angle of water droplets on an oil-infused etched aluminum surface versus time after exposure to hydrochloric acid.

Time (min)	Sample 7	Sample 8	Average
0	86.0	88.1	87.0
15	94.9	87.6	91.3
60	68.0	78.1	73.0
1440	0	0	0

Table 5. Contact angle of water droplets on an oil-infused etched aluminum surface (Teflon coated) versus time after exposure to hydrochloric acid.

Time (min)	Sample 15	Sample 16	Average
0	107.0	86.2	96.6
60	85.5	90.1	87.8
1440	131.2	116.7	123.9

2.5.4. Immersion liquid - Sodium hydroxide solution

Sodium hydroxide, a strong base, was also used to characterize the oil infused surface's resilience to basic media. A concentration of 0.6 molarity was used for these tests to be consistent with the acid resistance experiments. The sodium hydroxide (NaOH) tests followed the same procedure as the HCl tests. The measured contact angles for the etched aluminum and Teflon coated etched aluminum samples are shown in Tables 6 and 7 respectively.

The etched aluminum samples looked visually different after a 24 hour NaOH soak, as seen in Figure A13 in the appendix. NaOH removed the porous layer that the oil was trapped within, and created a new layer on the surface of aluminum. Though visually different than the HCl etched layer, this new layer absorbed water into its matrix, which results in a contact angle of 0° (Table 6).

Table 6. Contact angle of water droplets on an oil-infused etched aluminum surface versus time after exposure to sodium hydroxide.

Time (min)	Sample 13	Sample 14	Average
0	74.8	78.7	76.7
15	45.4	51.6	51.6
60	0	0	0
1440	0	0	0

For the Teflon coated samples the contact angle reaches an average of ~65° (Table 7) after the NaOH exposure. This nonzero contact angle cannot with certainty be attributed to the presence of the Teflon layer or an infused oil layer. Visual observations indicate that the Teflon layer is mostly intact, but no sheen from the oil layer can be seen. Additionally, the Teflon layer appears to be separating from the sample as NaOH reacts with the structure beneath the Teflon layer. At longer time periods the Teflon layer could likely detach from the sample. Pictures of this surface are included in the appendix (Figure A14).

Table 7. Contact angle of water droplets on an oil-infused etched aluminum surface (Teflon coated) versus time after exposure to sodium hydroxide.

Time (min)	Sample 17	Sample 18	Average
0	95.4	85.7	90.6
60	44.3	14.2	29.2
1440	64.1	67.8	65.9

2.5.5. Immersion liquid - Acetone

The last fluid used in these experiments was acetone, which is a common solvent used for cleaning. Experiments were conducted in closed and sealed containers to prevent the evaporation of the acetone in the bath. The etched aluminum samples were soaked in acetone for 24 hours, after which some samples were allowed to sit in open air for 24 hours and then submerged for an additional seven days. Contact angles were measured at 15 minutes, 60 minutes, 24 hours, after 24 hours of open air, and after 7 days of continuous soak. The Teflon coated etched aluminum samples were soaked for 24 hours with contact angles measured at the end of the 24 hour soak. The data for the etched aluminum and Teflon coated etched aluminum surfaces are shown in Tables 8 and 9 respectively.

There is not much consistency in the results (Table 8), with contact angles ranging from hydrophobic to hydrophilic at the 24 hour mark. The properties of acetone can explain the large variance in the contact angles. Acetone is an organic compound miscible in olive oil. This will produce a solution of acetone and olive oil that can interact with the etched aluminum's surface. Acetone is amphipathic, comprised of both hydrophilic and hydrophobic molecules, which could explain the variation in contact

angles along the surface. The wettability of the aluminum sample could vary based on how the acetone molecules arrange themselves within the etched pores. Samples that were exposed to air for 24 hours showed a marginal decrease in contact angle. Acetone that was present in the etched matrix could have displaced the oil in the matrix, and then evaporated changing the surface to be more hydrophilic, which it originally was. For the seven day soak tests, no significant difference in contact angle was observed between samples submerged for 24 hours and samples submerged for seven days. More research should be conducted to study this phenomenon to determine the cause for this variance.

The Teflon coated etched aluminum samples followed a similar trend of increasing contact angle after the 24 hour soaking period. Acetone most likely mixed with the oil to remove it from the surface of these samples. The Teflon coated samples take much longer to absorb the oil into their matrix and exhibit less absorption than the etched samples. This could have led to acetone removing the olive oil from the Teflon coated samples and explains the return to the original contact angle of a Teflon coated sample. Three of the four samples approached contact angles that were close to the contact angle of a water droplet on a Teflon coated sample, ~155°-160°. The sample that did not follow this trend, Sample 20, appeared visually different than the other samples. This difference could have been due to some variation during the etching or coating procedure. Pictures of the samples after the test are included in the appendix (Figure A15, A16).

Table 8. Contact angle of water droplets on an oil-infused etched aluminum surface versus time after exposure to acetone.

Time (hour)	Sample 3	Sample 4	Sample 9	Sample 10	Sample 25	Sample 26	Average
0	78.1	78.7	77.8	80.9	85.4	81.3	80.4
0.25	87.0	130.9	-	-	-	-	108.9
1	129.2	131.5	127.2	84.7	-	-	118.2
24	137.1	130.0	35.1	36.8	115.4	73.1	87.9
24, post acetone	126.3	122.8	14.1	27.0	-	-	72.5
168	137.7	108.7	-	-	-	-	123.2

Table 9. Contact angle of water droplets on an oil-infused etched aluminum surface (Teflon coated) versus time after exposure to acetone.

Time (hour)	Sample 19	Sample 20	Sample 27	Sample 28	Average
0	76.4	89.7	78.1	77.5	80.4
24	142.9	123.0	153.2	153.2	143.0

Chapter 3

Fluid retention in etched aluminum surfaces in the presence of liquid shear

Chapter 2 detailed studies to understand the chemical resistance of the etched aluminum surfaces; these involved experiments with static fluids. This chapter details studies to quantify the ability of etched aluminum surfaces to retain a liquid film (in its texture) in the presence of shear flows. These studies are directly relevant to the development of technologies related to oil-gas flow assurance. The applications discussed in Chapter 1 hinge on the success of the surfaces in maintaining a stable water film.

Three sets of experiments were conducted and are reported presently. The first experiment quantifies the ability of the etched aluminum surface to retain oil in the presence of water flow. The second experiment quantifies the ability of the etched aluminum surface to retain water in the presence of oil flow. Both these experiments were conducted in a custom built flow loop described in Section 3.1. The third experiment quantifies the ability of the surface to retain oil when subject to impingement of a high pressure water stream.

3.1. CUSTOM BUILT FLOW LOOP TO MEASURE THE STABILITY OF A FLUID FILM UNDER SHEAR FLOW.

Figure 8 shows a schematic of the recirculating flow loop that was used to flow water through a test section that the oil infused samples were housed in. The flow loop included a clog-resistant circulating centrifugal pump (Jabsco Model 11810-003), transparent plastic tubing, globe valves, pressure gauges (Winters PEM Series 0-15 psi pressure gauge), a flow meter (Uxcell HQ-A168 Hall Effect flow meter), a reservoir, and the test section. The pump speed and output flow was controlled by a Variac; the pump

had a maximum output of 9.6 GPM at 4.3 psi for water. The flow loop had two main lines from the pump outlet, a return to the reservoir and a line to the test section. The globe valves were used to control the flow rate to the test section. The pressure gauges were analog dial pressure gauges and the flow meter was a digital rotary flow meter. The reservoir was a 30 gallon drum.

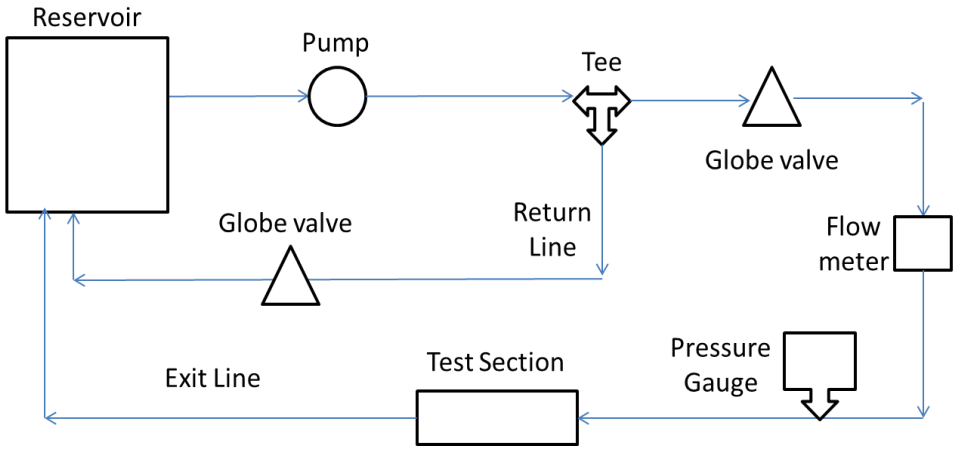

Figure 8. Schematic of flow loop used for shear flow experiments.

The test section was constructed of transparent acrylic (for flow visualization) and had three slots on the bottom plate to house the samples during flow tests. Three corresponding ports were created on the top of the test section to allow for placement of the samples; these ports were clamped down during tests and sealed with a gasket. The middle port was not used during tests and was instead used as an air release line to allow trapped air bubbles to escape the test section. The test section was 24 inches long with inner cross section dimensions of 3 inches (width) by 1 inch (height).

Figure 9 shows the pump, Variac, power supply for the flowmeter, globe valve, upstream of test section, the tubing section that returns to the reservoir, and the tubing section to the test section. Figure 10 shows the pressure gauge, flow meter, test section, reservoir, and air return line that was used to remove air bubbles from the test section.

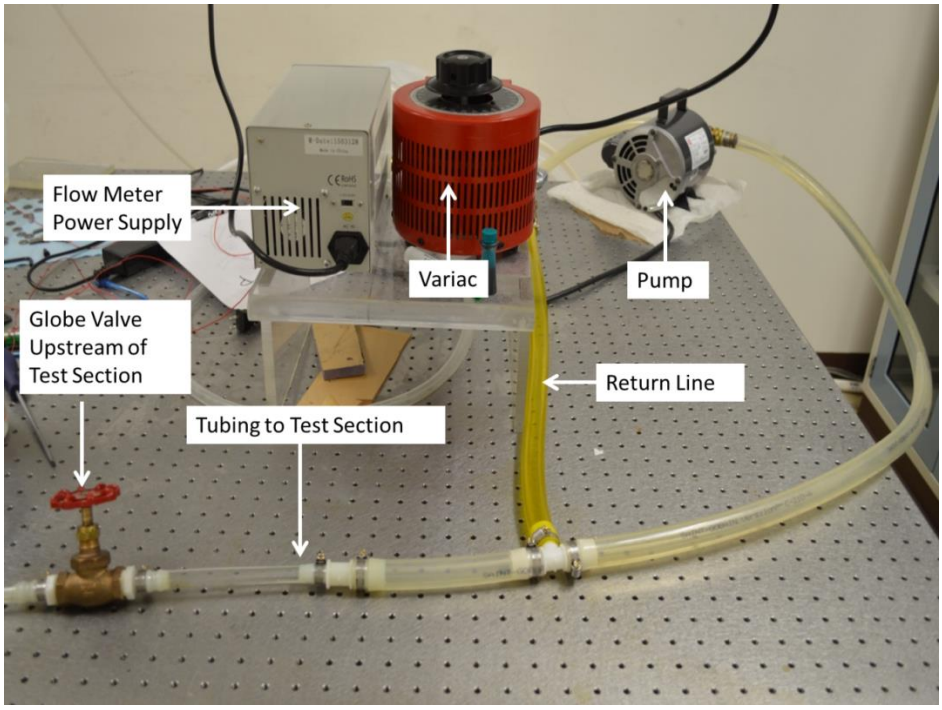

Figure 9. Flow loop upstream of test section.

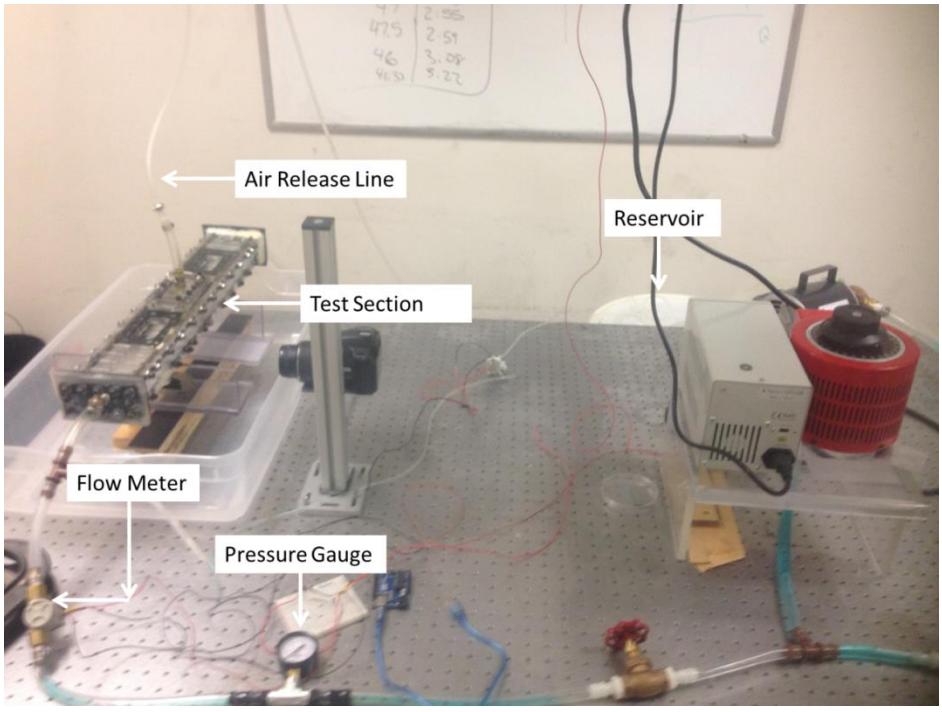

Figure 10. Flow loop including instrumentation and test section.

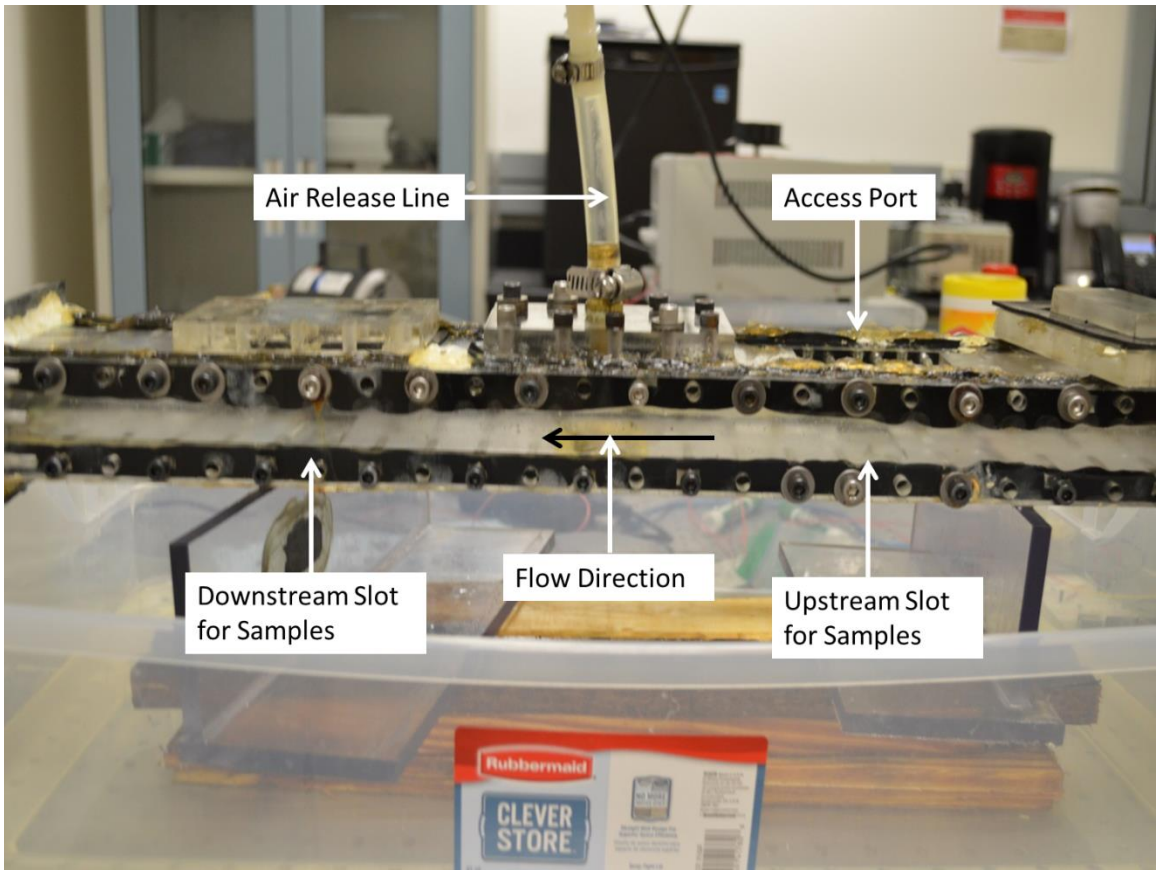

Figure 11. Side view of the test section.

It is important to note that this work examined flow in a rectangular cross section, instead of a circular cross section. This was necessitated by the use of rectangular test samples. The velocity pattern in a rectangular cross section is more complex than that in a circular cross section. Analytical solutions exist for flow in a rectangular channel. The velocity profile for flow through a rectangular cross section is [19]:

$$u(y,z) = \frac{16a^2}{\mu\pi^3}\left(-\frac{d\hat{p}}{dx}\right)\sum_{i=1,3,5\ldots}^{\infty}(-1)^{(i-1)/2}\left[1-\frac{\cosh(\frac{i\pi z}{2a})}{\cosh(\frac{i\pi b}{2a})}\right]\times\frac{\cos(\frac{i\pi y}{2a})}{i^3} \qquad (2)$$

where a and b are the width and height of the cross section, $\left(-\frac{d\hat{p}}{dx}\right)$ is the pressure gradient, and μ is the dynamic viscosity of the liquid [19, 20]. The total flow rate through the cross section (which is directly measured) can be obtained by integrating the above equation to obtain:

$$Q = \frac{4ba^3}{3\mu}\left(-\frac{d\hat{p}}{dx}\right)\left[1 - \frac{192a}{\pi^5 b}\sum_{i=1,3,5\ldots}^{\infty}\frac{\tanh(\frac{i\pi b}{2a})}{i^5}\right] \quad (3)$$

which uses the same variables as Equation 1 [19, 20, 21].

Based on the pump's maximum operating flowrate of 9.6 GPM, some of the flow characteristics for the fluids used in the shearing experiments will be discussed here. Tap water at room temperature (density: 1000 kg/m^3, viscosity: 1.004 cSt) and mineral oil (density: 880 kg/m^3, viscosity: 10 cSt) at room temperature were the two fluids used. The maximum Reynolds Number (Re) was calculated using:

$$Re = \frac{\rho V D_h}{\mu} \quad (4)$$

which yielded a Re of 11900 for water and a Re of 1190 for mineral oil. In Equation 4, ρ is the fluid density, V is the fluid velocity, D_h is the hydraulic diameter of the pipe (Equation 7), and μ is the dynamic viscosity of the fluid. The flow regimes would be turbulent flow for the water and laminar flow for the mineral oil. Rearranging and using Equation 3 with the assumption that maximum flowrate of 9.6 GPM can be achieved, the maximum pressure drops are predicted to be 6.5x10^{-4} (psi) for water and 5.7x10^{-3} (psi) for mineral oil. The entrance length was calculated as 21.3 inches for turbulent water flow and 89.4 inches for laminar mineral oil flow using Equation 5 for laminar flow:

$$L_h = 0.05(Re)D_h \tag{5}$$

and Equation 6 for turbulent flow:

$$L_h = 1.359(Re^{1/4})D_h \tag{6}$$

where L_h is the entrance length, *Re* is Reynolds Number, and D_h is the hydraulic diameter of the pipe (Equation 7) [22, 23]. In order to predict the maximum flowrate through the test section a pressure drop value is required. However the pressure drops needed for Equation 3 for this flowrate are too small to measure using the dial pressure gauge in our test setup. To determine an expected pressure drop to be used in Equation 3, the Moody chart, hydraulic diameter, the friction factor, and the pressure drop equation for pipe flow was used. The hydraulic diameter [14, 22] was used to enable the use of correlations typically used for circular cross sections.

$$D_h = \frac{4A}{P} \tag{7}$$

D_h is the hydraulic diameter, *A* is the cross-sectional area, and *P* is the wetted perimeter of the cross-section. The Moody chart was used to estimate the friction factor based on Reynolds Number and dimensionless roughness, estimated as ϵ/d. Roughness, ϵ is dependent upon the material and the fabrication process.; a value of 0.0025 mm was used for the acrylic test section. The hydraulic diameter estimate using equation 7 was 0.038 meters [14, 22, 24, 25]. The equation to predict the pressure drop is:

$$\Delta P = f\frac{\rho L}{2D_h}V^2 \tag{8}$$

where ΔP is the pressure drop, *f* is the friction factor, *L* is the length of the pipe, D_h is the hydraulic diameter of the pipe (Equation 7), *V* is the average velocity of the fluid, and ρ

is the density of the fluid [22, 23, 24, 25]. Using Equations 5 through 8, the predicted pressure drops for the test section were 6.1×10^{-4} (psi) for water and 5.4×10^{-4} (psi) for mineral oil. Using these estimated pressure drops in Equation 3 yielded maximum estimated flowrates of 9.0 GPM for both fluids. The flow characteristics for the water flow and oil flow experiment are included in Table A1 in the appendix.

The procedure for the experiments to displace oil with water flow is described ahead. 2 inch by 1 inch etched aluminum wafers were infused with olive oil and placed in test section. Next, all inlet and outlet tubing sections were secured within the reservoir; it was verified that the inlet was below the fluid level. When the inlet is not below the fluid level, the pump runs dry, and this can cause pump impeller failure. The globe valve to the test section was closed and the test sections clamps were securely fastened to ensure there was no leakage. Next, the pump was turned on and allowed to run for a few minutes before opening the globe valve to the test section. The globe valve was then opened partially so that the test section could slowly fill, to avoid a large impulse of fluid entering the test section which could dislodge the samples from their slots. Once the test section was half full, the globe valve was opened fully to allow for the rest of the test section to fill up. During this time it was necessary to lean the test section slightly to allow any trapped air bubbles to escape. The flow was allowed to continue for the pre-designated length of time. At the conclusion of the experiment, the sample was removed from the test section and allowed to dry.

3.2. RETENTION AND STABILITY OF OIL FILMS UNDER WATER SHEAR.

This section describes the experiments to study the retention of oil under the action of water shear. These experiments were conducted on etched aluminum surfaces

and Teflon coated etched aluminum surfaces. Both these surfaces were infused with olive oil. The samples were exposed to tap water flowing at 8 GPM for 24 hours. Contact angle measurements (water droplets on oil-infused surfaces) in Table 10 and Table 11 are for etched aluminum and Teflon coated etched aluminum respectively.

Overall, there was no significant change in the contact angle for any sample. This indicates that the surfaces can withstand water flow speeds of at least 0.26 m/s (which corresponds to a Re of 9910). The approximate shear stress at the surface can be calculated based on the velocity profile in Equation 2 as per Equation 9 below, and is 0.038 Pa for the water flow experiments. It was visually observed that excess oil that had not rolled off the surface before the test was present in the water as the test section was being filled before the test. The location of the substrate in the test section did not have a significant effect on the contact angle of the samples. Pictures of the samples after the tests are included in the appendix (Figure A21, A22).

$$\tau = \mu \frac{du}{dy} \tag{9}$$

Table 10. Contact angle measurements of water droplets on oil-infused etched aluminum surfaces after exposure to water flow.

Location in test section	**Upstream**	**Downstream**	**Downstream**	**Upstream**	**Average**
Time (hour)	Sample 5	Sample 6	Sample 11	Sample 12	-
0	76.0	76.0	88.0	85.0	81.3
24	69.2	84.2	85.9	79.1	79.6

Table 11. Contact angle measurements of water droplets on oil-infused etched aluminum surfaces (Teflon coated) after exposure to water flow.

Location in test section	Downstream	Upstream	Average
Time (hour)	Sample 21	Sample 22	-
0	81.8	84.4	83.1
24	89.3	88.5	88.9

3.3. RETENTION AND STABILITY OF WATER FILMS UNDER OIL SHEAR.

The second set of experiments used the above setup and similar procedures, but instead used oil flow to shear off water infused in the surface. Contact angle measurements with water droplets cannot be used on the water infused samples, if water is retained in the sample. Therefore, mass measurements were used to determine if the water in the surface was removed, and replaced by oil.

3.3.1. Experimental setup and procedures

The experimental setup and procedure were similar to the previous experiment. The differences in the setup were the flowing fluid and the tubing size. The flowing fluid was light machine tool spindle mineral oil ISO grade 10, which is approximately ten times more viscous than tap water. The tubing size on one stretch of tubing was adjusted to prevent damage to the pump from the more viscous oil. The procedure was similar to the previous experiment; the changes involved the flowrate, post test sample handling, and quantifying results. The water infused samples were weighed after fabrication and water infusion; excess water was allowed to roll off before weight measurements. The

samples were then placed in the test section and exposed to oil flow at 4 GPM for 12 hours. After the test, the samples were removed and the excess fluid was drained off. The samples then were exposed to a gentle heating process and weighed after they cooled. The gentle heating process involved the sample sitting on a hot plate at 70° C for a minimum of four hours to allow any water in the texture to evaporate. A sub-boiling temperature was chosen so as to not harm the etched structure, as previous experiments had shown that boiling water can affect the surface.

3.3.2. Results - Stability of water films under oil shear

The oil flow experiments were conducted solely on etched aluminum surfaces infused with water, no Teflon coated surfaces were used in this experiment. This was due to the fact that Teflon surfaces cannot be infused with water. The results for mass change and contact angle measurements during the stages of the experiment are shown in Table 12 and Table 13 respectively. The mass measurements given are the percent mass of oil absorbed compared to original mass of water absorbed; additional data is provided in the appendix (Tables A2–A4). The mass measurements corroborated the visual observations that the flowing oil removed some of the water from the surface and replaced it. After the flow test, and after heating it was seen that the mass of the sample had increased from the original mass. The mass increase was due to oil absorbed into the sample's etched matrix. The oil mass absorbed by the samples ranged from 40% to 107% of the water mass absorbed by the samples before the flow test. Four samples were used in two trials of the oil shear flow experiment. Samples 43 and 44 were used in trial 1 and Samples 45 and 46 were used in trial 2. The two samples placed in the upstream slot were Samples 43 and 45, while Samples 44 and 46 were placed in the downstream slot. The upstream samples

absorbed more oil than their downstream counterpart in both trials; this could be due to the additional turbulence near the upstream slot. The increased turbulence at the surface could cause the oil to displace more water in the surface's texture. The average percentage mass of oil absorbed in each trial was 86.6% in the first trial, and 41.4% in the second. The higher oil absorption in the first trial could be due to those samples initially absorbing 34% less water (on average) than the samples in the second trial. The smaller amount of water in the sample's matrix allowed for the flowing oil to remove and replace water more easily in Samples 43 and 44 than in Samples 45 and 46.

Once it was determined that shear oil flow could remove and replace water in the surface's matrix, contact angle measurements were recorded. Baseline contact angle measurements of a water droplet on an etched aluminum surface infused with mineral oil were conducted using Samples 47 and 48. The baseline contact angles are compared to the water droplet contact angles for Samples 43 to 46, and the results are shown in Table 13. The average contact angle for Samples 47 and 48 was 80°, while the average contact angle for the Samples 43 to 46 after the shear oil flow experiment was 119.5°. The baseline contact angles are lower than the post oil flow contact angles because the water droplets are interacting with a surface that has more oil in it. The droplets in the baseline measurements are subject to more of a liquid-liquid (oil-water) interaction than the droplets on the shear oil flow surfaces. An example of this can be seen in Figure A7 in the appendix, where a water droplet is deposited on a pool of oil on the surface. When a water droplet is deposited on a surface flooded with oil the droplet will spread on the pooled oil rather than bead.

The surfaces after the oil shear experiment are not completely infused with oil, which leads to an interaction similar to the interaction of the water droplet with the Teflon coated samples. On such surfaces, the water droplet is subject to more of a liquid-

surface interaction than the water droplet in the baseline samples. This leads to beading up and decreased wettability when compared to the baseline measurements. An etched aluminum surface, not completely infused with oil will have lower wettability compared to a surface with oil completely infused. This is due to the water droplet interacting with more of the roughness causing elements. On the other hand, when the surface is completely infused with oil, the droplet interacts with less of the roughness causing elements and experiences more of a liquid-liquid (oil-water) interaction.

Overall, these preliminary experiment shows that the textured surface can be inadequate in to maintaining a water film under oil shear flow at flow velocities 0.13 m/s (Re of 500). Pictures of the surfaces after the experiment are included in the appendix (Figure A23).

Table 12. Percentage mass of oil absorbed in the texture after the oil flow experiments, compared to the original mass of water absorbed.

Sample	Oil Absorbed
43	107.4%
44	65.7%
45	42.9%
46	40.0%

Table 13. Contact angles of water droplets on etched aluminum surfaces after being exposed to flowing mineral oil.

Sample	Oil Bath	After Flow
43	-	114.2
44	-	116.7
45	-	113.9
46	-	133.4
47	76	-
48	84	-

3.4. RETENTION AND STABILITY OF OIL FILMS UNDER A HIGH PRESSURE WATER JET

The third set of experiments evaluated the ability of the surfaces to hold oil in the presence of a high pressure water jet impinging on the sample. The objective of this experiment was to determine the pressure at which the oil trapped in the etched aluminum's matrix is removed. Oil removal was quantified using mass loss measurements and contact angle measurements.

3.4.1. Experimental setup and procedure

The main components used in these experiments included a Briggs and Stratton 4000 psi pressure washer with a 0 degrees jet nozzle. A garden hose was connected to the compressor of the pressure washer as the main water supply. The outlet of the pressure washer was a hydraulic hose that connected to a small length of pipe with a pressure gauge. The pipe was then connected to the wand of the pressure washer where the water

stream would exit through the jet nozzle. The connections before the pressure washer's compressor were made using a threaded connection; while all connections after the compressor utilized quick connect connections. The pressure gauge was an analog dial gauge, which allowed for a pressure reading before the wand.

The etched aluminum surfaces used in this experiment were 2 inch by 2 inch, and were prepared using process described earlier. The samples were infused with olive oil (density: 910 kg/m^3, viscosity: 91.5 cSt at 22° C) before being sprayed with the high pressure water stream. Samples were secured to a wooden board and sprayed for three minutes at increasing pressures. The pressures used in this experiment ranged from 50 psi to 3400 psi, which were the minimum and maximum outputs of the pressure washer. Two samples were used for every value of pressure. The distance from the tip of the wand to the sample was 24 inches. Post spraying, the mass of the samples was measured after the samples were subjected to a gentle heating process to get rid of water. The samples were weighed at discrete points throughout the experiment: after fabrication, after being immersed in oil and letting the excess oil roll off, after being sprayed, and after being heated. Contact angle measurements with water droplets were taken after being exposed to oil and after the gentle heating process.

3.4.2. Results - Stability of oil films under high pressure water impingement

The oil mass loss and the contact angle measurements are presented in this section. These oil loss results can be seen in Figure 12. The mass loss measurements show that at 50 psi and 100 psi impingement pressures, 38.8% and 28.3% of the oil added to the sample was displaced. For pressures greater than 200 psi the oil loss experienced is much higher, ranging from 51.2% to 79.4% oil loss. There is no apparent trend in these

measurements, but one would expect that higher pressures would remove more oil. It is noted though that the size of the water stream and the flowrate also increased with pressure. As the stream size grew, a large amount of water dispersion in the form of mist was observed during the tests. The larger streams spread the impinging force on the sample over a larger area, while the smaller streams were more concentrated on the sample. This observation could explain the variation in the data and the somewhat surprising result that smaller pressures removed similar amounts of oil as very high pressures.

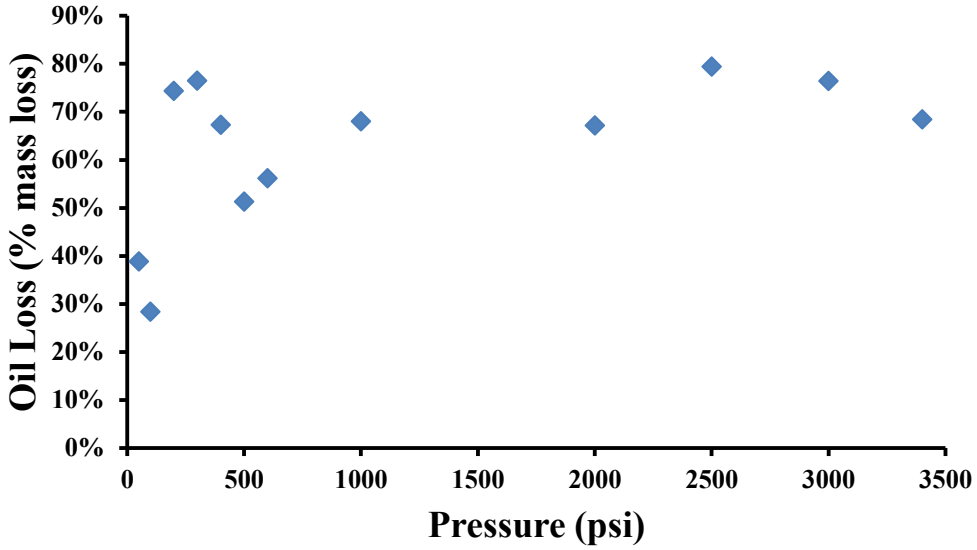

Figure 12. Fraction of oil loss from an oil infused surface as a function of the pressure of the impinging water jet.

The results for the contact angle measurements are shown in Figure 13. At 50 psi the contact angle does not show any change after the impingement tests. Based on the previous experiments, it appears that the mass loss at 50 psi could have been due to excess oil on the surface and not due to removal of oil trapped in the texture. The trend for the contact angle measurements follows a similar trend as the mass loss

measurements, with the maxima for both measurements aligning at the same pressures: 200, 300, and 2500 psi. As more oil is removed from the surface, the contact angle tends to increase. This phenomenon was also observed in the oil shear flow experiments.

The increase in contact angle indicates that the water droplet-surface interaction became more hydrophobic, which will reduce adhesion. This could be explained by the reduced oil layer in the surface's texture, which allows for increased interaction between the water droplet and the roughness causing elements on the surface. This increased droplet-roughness interaction, as well as the decrease in the amount of oil retained in the surface's texture leads to the increase in contact angle.

Overall, the pressure impingement experiments show that the etched aluminum samples show modest ability to retain oil under high pressure impinging water flows. Pictures of the samples after the tests are shown in the Appendix (Figure A25-A29).

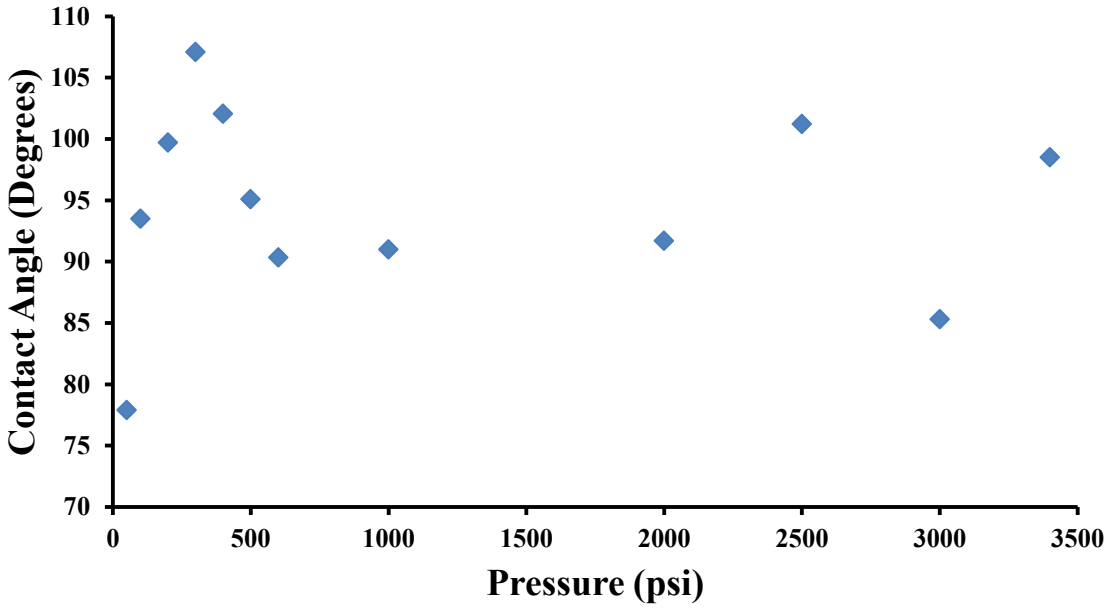

Figure 13. Post experiment contact angles of water droplets on an oil infused surface as a function of the pressure of the impinging water jet.

Chapter 4

Conclusions and future work

This dissertation presented qualitative and quantitative experimental results to determine the ability of etched aluminum surfaces in retaining liquid in surface textures. Key findings are summarized and future work is discussed in this section.

4.1. SIGNIFICANT FINDINGS

The significant findings and key contributions of this work are as follows:

1. Etched aluminum surfaces retain oil in room temperature water environments. However, they are unable to retain oil under boiling water conditions, presumably because bubble nucleation displaces oil from the texture.
2. Etched aluminum surfaces do not have significant chemical resistance to high concentrations of acidic or basic media. The durability of these surfaces in milder acidic or basic solutions needs to be evaluated.
3. The etched aluminum surfaces can retain oil in the presence of shear water flow. Stable oil films were observed at water velocities as high as 0.26 m/s, which translates to a Re of 9910.
4. Etched aluminum surfaces were not able to retain water under oil flow at a flow speed (of oil) of 0.13 m/s (Re of 500). It is noted that the oil was 10 times more viscous than water. The ability of such surfaces to retain water at lower velocities needs to be evaluated.
5. The etched aluminum surfaces displayed loss of oil under the action of a water jet impinging at pressures exceeding 200 psi.

4.2. FUTURE WORK

The following refinements and extensions are proposed for future work on this topic.

- The present flow experiments were preliminary in nature. The flow loop for future experiments can be redesigned based on the findings of the present experiments, to provide more useful information about the phenomena occurring at the solid-liquid interface.
- The present experiments established water loss under oil flow, but did not isolate a threshold flow velocity at which water loss starts becoming significant. This should be a focus of future experiments.
- Similarly, the present experiments established that the surface can retain oil films under water flow. However, this work does not quantify the velocity at which water will shear off oil. Experiments with higher water flow speeds are essential to quantify this.
- The threshold pressure above which oil loss starts becoming significant needs to be quantified by more careful pressure wash experiments.
- The mechanisms underlying liquid removal by shear flow or by high pressure jet impingement need to be studied in more detail. This is possible via experimental approaches (visualization) or via computational approaches.
- The role of electrowetting in enhancing the adhesion of water films to the surface needs to be examined. The experimental setup can be modified to provide electrical voltages for such experiments.

Appendix

Table A1. Flow characteristics of shear flow experiments.

Flow Characteristics	Water	Mineral Oil
Q (GPM)	8	4
Re	9910	500
Flow Regime	Turbulent	Laminar
Pressure Drop (psi)	5.4×10^{-4}	2.4×10^{-3}
Entrance Length (inches)	20.3	37.3

Table A2. Mass measurements corresponding to the oil flow experiments. All measurements are in grams.

Sample	Pre Water	Post Water	Post Oil Flow	Post Heat	Time (hour)
43	12.39	12.42	12.44	12.41	12
44	11.83	11.86	11.88	11.86	12
45	11.94	12.03	12.01	11.97	12
46	11.79	11.88	11.86	11.82	12

Table A3. Mass of liquid infused in surface in the oil flow experiments. All measurements are in grams.

Sample	Water Added	Water + Oil	Oil Added	Water Lost	Time (hr)
43	0.027	0.05	0.041	0.029	12
44	0.035	0.052	0.046	0.023	12
45	0.091	0.073	0.057	0.039	12
46	0.09	0.068	0.053	0.036	12

Table A4. Percentage change in liquid mass compared to original water infused in the oil flow experiments.

Sample	Water Added	Post Spray	Post Heat	Oil Absorbed
43	100%	85.2%	51.9%	107.4%
44	100%	48.6%	31.4%	65.7%
45	100%	-19.8%	37.4%	42.9%
46	100%	-24.4%	41.1%	40.0%

Table A5. Mass measurements of pressure wash experiments. All measurements are in grams.

Sample	Pre Oil	Post Oil	Post Spray	Post Heating	Pressure (psi)
1	22.421	22.545	22.496	22.462	1000
2	17.434	17.544	17.494	17.468	1000
3	18.935	19.069	19.012	18.985	2000
4	19.071	19.18	19.132	19.102	2000
5	21.509	21.619	21.56	21.528	2500
6	17.842	17.9549	17.901	17.869	2500
7	19.432	19.567	19.485	19.468	3000
8	18.484	18.62	18.528	18.512	3000
9	20.942	21.036	20.994	20.967	200
10	21.1519	21.229	21.203	21.171	200
11	20.914	20.994	20.938	20.932	300
12	21.12	21.193	21.153	21.138	300
13	21.38	21.459	21.414	21.402	400
14	22.673	22.8005	22.736	22.721	400
15	20.916	21.059	21.004	20.9859	500
16	20.816	20.958	20.905	20.885	500
17	22.511	22.614	22.569	22.555	600
18	20.609	20.751	20.693	20.673	600
19	19.158	19.678	19.612	19.603	100
20	19.067	19.263	19.219	19.18	100
21	19.098	19.28	19.227	19.204	50
22	20.242	20.37	20.336	20.324	50
23	22.429	22.513	22.467	22.453	3400
24	22.019	22.0999	22.058	22.047	3400

Table A6. Difference in mass in pressure wash experiments at every step. All measurements are in grams.

Sample	Pre Oil	Post Oil	Post Spray	Post Heating
1	0	0.124	-0.049	-0.034
2	0	0.11	-0.05	-0.026
3	0	0.134	-0.057	-0.027
4	0	0.109	-0.048	-0.03
5	0	0.11	-0.059	-0.032
6	0	0.1129	-0.0539	-0.032
7	0	0.135	-0.082	-0.017
8	0	0.136	-0.092	-0.016
9	0	0.094	-0.042	-0.027
10	0	0.0771	-0.026	-0.032
11	0	0.08	-0.056	-0.006
12	0	0.073	-0.04	-0.015
13	0	0.079	-0.045	-0.012
14	0	0.1275	-0.0645	-0.015
15	0	0.143	-0.055	-0.0181
16	0	0.142	-0.053	-0.02
17	0	0.103	-0.045	-0.014
18	0	0.142	-0.058	-0.02
19	0	0.52	-0.066	-0.009
20	0	0.196	-0.044	-0.039
21	0	0.182	-0.053	-0.023
22	0	0.128	-0.034	-0.012
23	0	0.084	-0.046	-0.014
24	0	0.0809	-0.0419	-0.011

Table A7. Percentage change in liquid mass compared to original oil added for pressure wash experiments. All measurements are in grams

Sample	Oil Added	Post Spray	Post Heat	Total Oil Lost	Oil Retained	Pressure (psi)
1	100%	-39.516%	-66.935%	-66.935%	33.065%	1000
2	100%	-45.455%	-69.091%	-69.091%	30.909%	1000
3	100%	-42.537%	-62.687%	-62.687%	37.313%	2000
4	100%	-44.037%	-71.560%	-71.560%	28.440%	2000
5	100%	-53.636%	-82.727%	-82.727%	17.273%	2500
6	100%	-47.741%	-76.085%	-76.085%	23.915%	2500
7	100%	-60.741%	-73.333%	-73.333%	26.667%	3000
8	100%	-67.647%	-79.412%	-79.412%	20.588%	3000
9	100%	-44.681%	-73.404%	-73.404%	26.596%	200
10	100%	-33.722%	-75.227%	-75.227%	24.773%	200
11	100%	-70.000%	-77.500%	-77.500%	22.500%	300
12	100%	-54.795%	-75.342%	-75.342%	24.658%	300
13	100%	-56.962%	-72.152%	-72.152%	27.848%	400
14	100%	-50.588%	-62.353%	-62.353%	37.647%	400
15	100%	-38.462%	-51.119%	-51.119%	48.881%	500
16	100%	-37.324%	-51.408%	-51.408%	48.592%	500
17	100%	-43.689%	-57.282%	-57.282%	42.718%	600
18	100%	-40.845%	-54.930%	-54.930%	45.070%	600
19	100%	-12.692%	-14.423%	-14.423%	85.577%	100
20	100%	-22.449%	-42.347%	-42.347%	57.653%	100
21	100%	-29.121%	-41.758%	-41.758%	58.242%	50
22	100%	-26.563%	-35.937%	-35.937%	64.063%	50
23	100%	-54.762%	-71.429%	-71.429%	28.571%	3400
24	100%	-51.792%	-65.389%	-65.389%	34.611%	3400

Table A8. Percentage change in oil mass, from oil infusion to post heat step versus pressure for pressure wash experiments.

Pressure (psi)	Total Oil Lost
50	41.76%
50	35.94%
100	14.42%
100	42.35%
200	73.40%
200	75.23%
300	77.50%
300	75.34%
400	72.15%
400	62.35%
500	51.12%
500	51.41%
600	57.28%
600	54.93%
1000	66.94%
1000	69.09%
2000	62.69%
2000	71.56%
2500	82.73%
2500	76.09%
3000	73.33%
3000	79.41%
3400	71.43%
3400	65.39%

Table A9. Contact angle measurements of pressure washed samples after heating.

Pressure (psi)	Contact angle
50	78.00
50	77.80
100	93.83
100	93.17
200	99.75
200	99.67
300	111.17
300	103.00
400	97.50
400	106.60
500	94.83
500	95.33
600	93.33
600	87.33
1000	92.75
1000	89.20
2000	91.40
2000	92.00
2500	101.20
2500	101.25
3000	89.00
3000	81.60
3400	104.10
3400	92.90

Table A10. Flowrate of the pressure washer for a given pressure.

Pressure (psi)	Flowrate (GPM)
1000	2.00
1500	2.50
2000	2.80
2500	3.20
3000	3.50
3500	3.70
4000	4.00

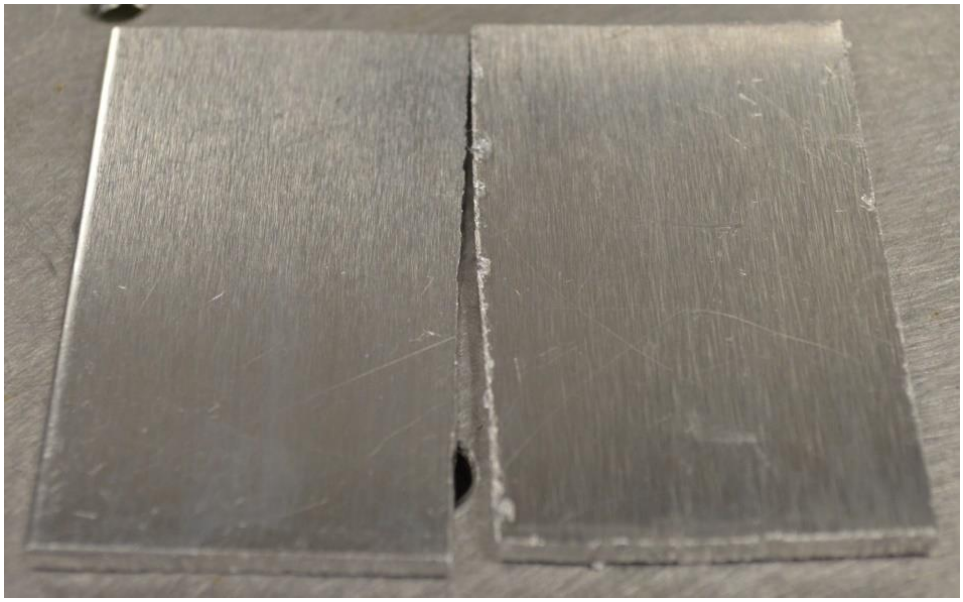

Figure A1. Polished aluminum sample.

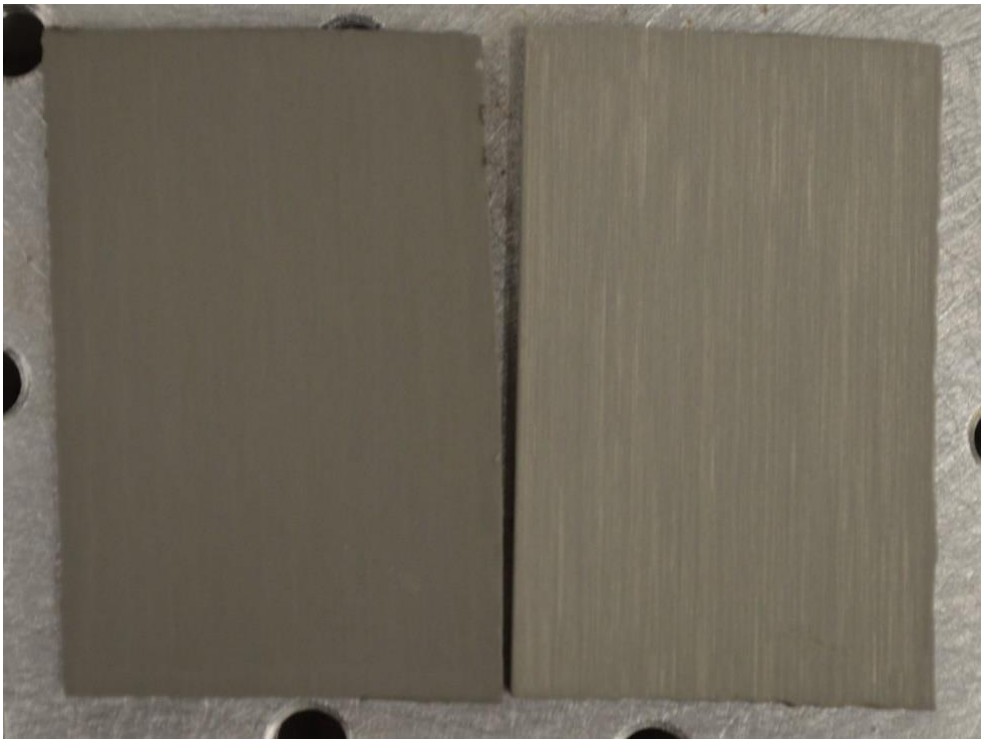

Figure A2. Aluminum etched in hydrochloric acid prior to liquid infusion.

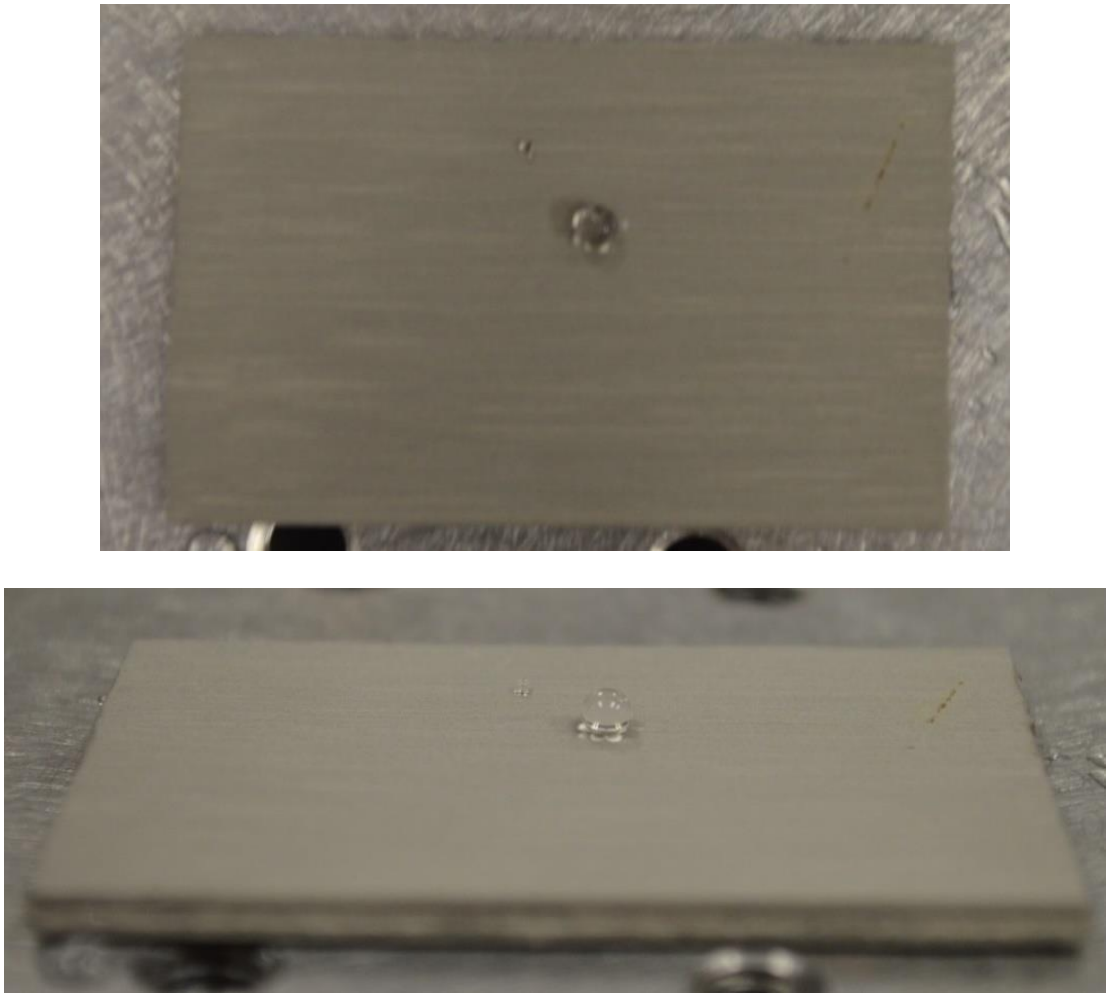

Figure A3. Water droplet resting on a Teflon coated etched aluminum surface.

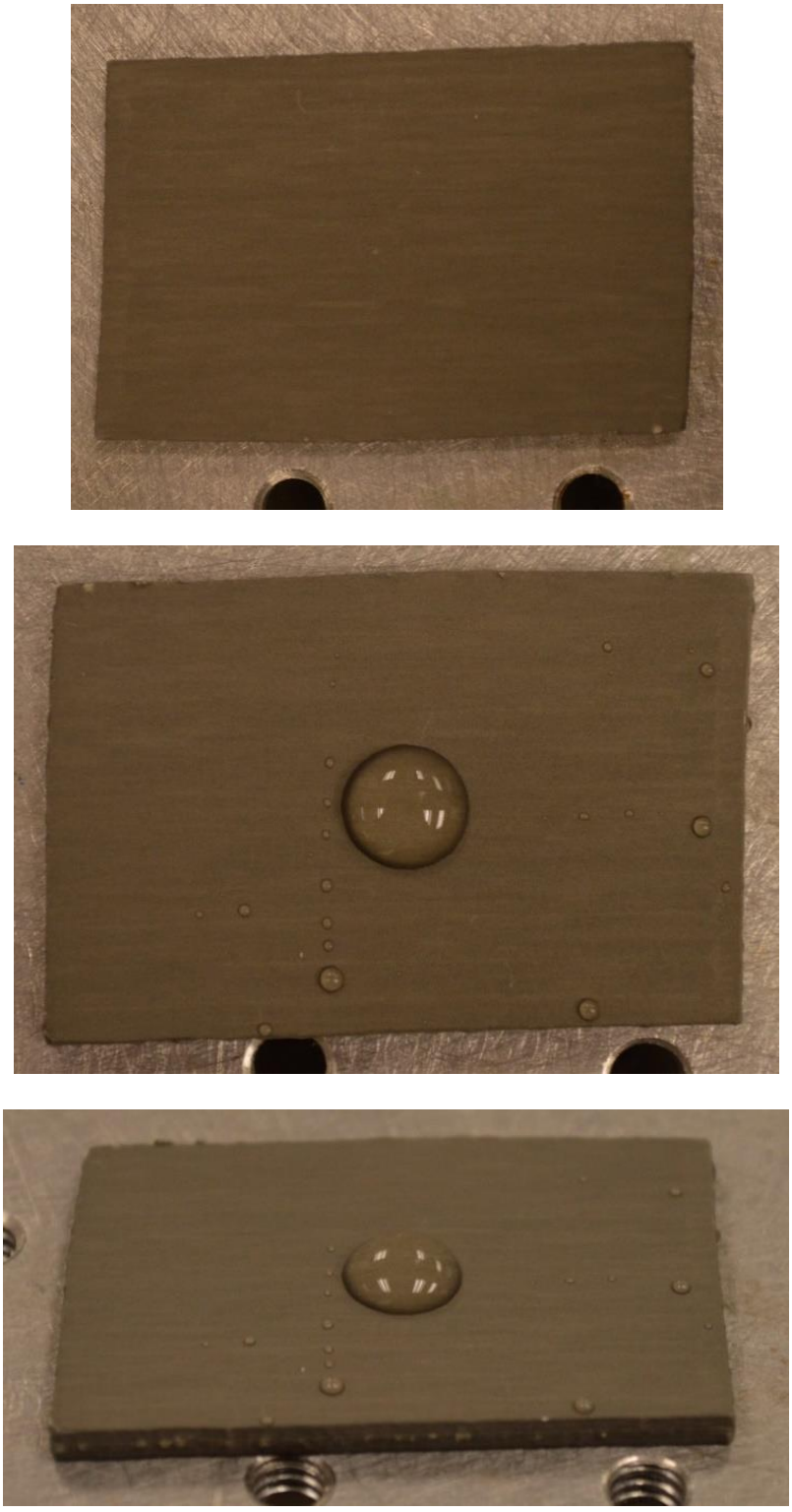

Figure A4. Oil infused etched aluminum sample with and without a water droplet.

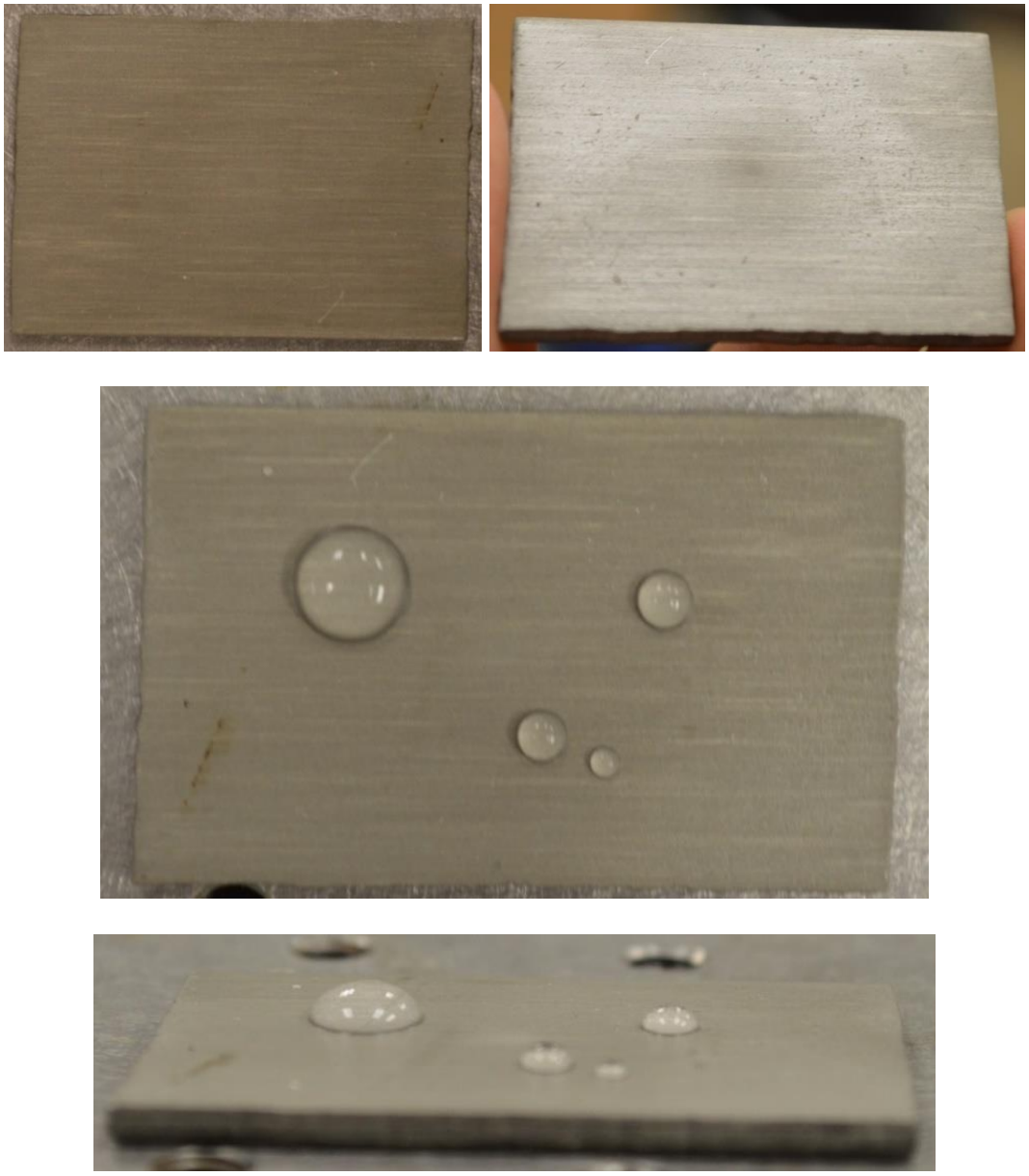

Figure A5. Oil infused Teflon coated samples with and without water droplets.

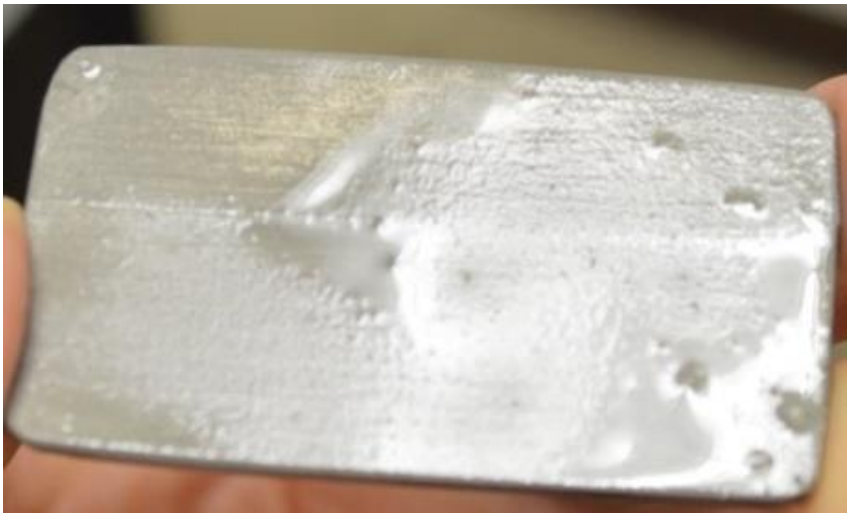

Figure A6. Oil infused sample with oil pooled on surface.

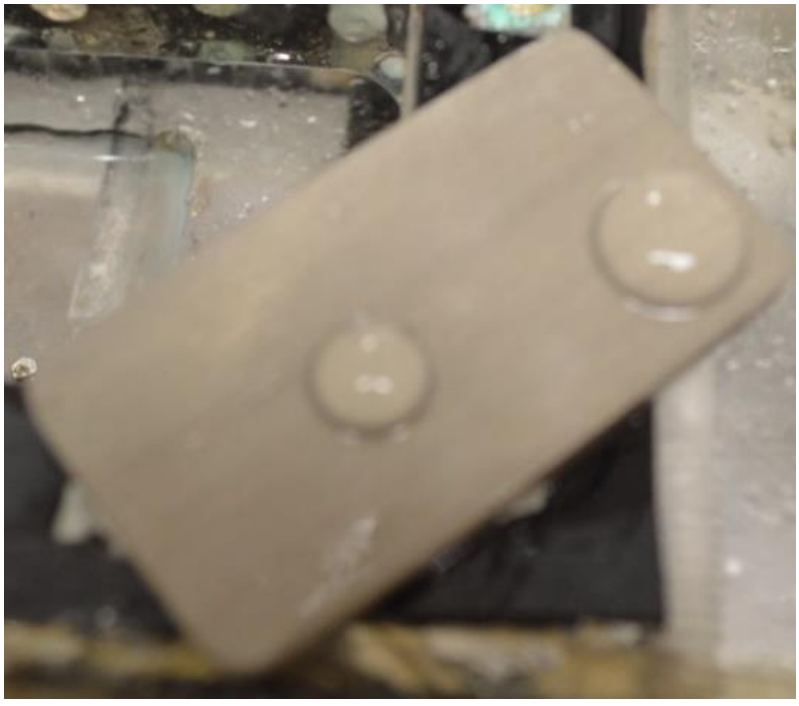

Figure A7. Water droplet spreading on oil pool present on oil infused surface.

Figure A8. Etched aluminum samples after tap water immersion.

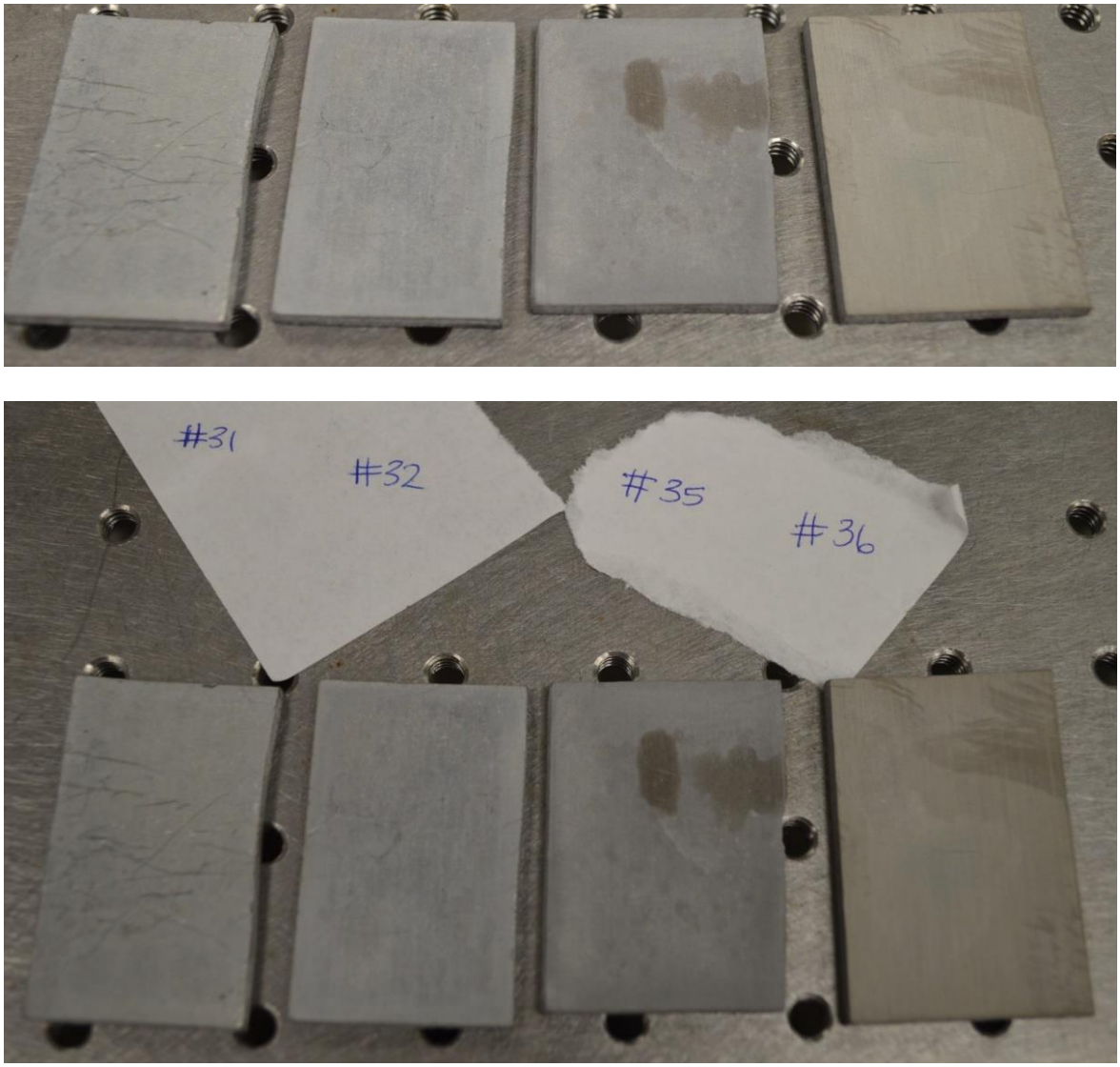

Figure A9. Etched aluminum samples after boiling water immersion.

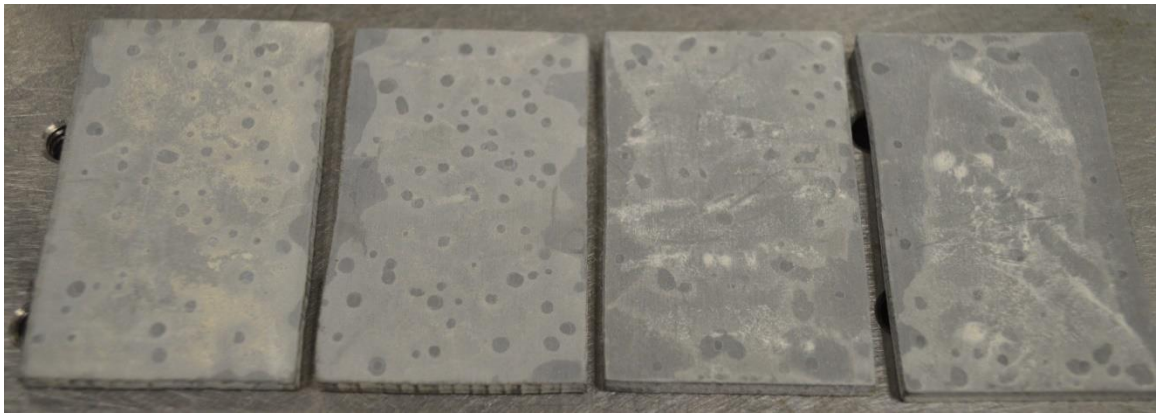

Figure A10. Teflon coated etched aluminum samples after boiling water immersion.

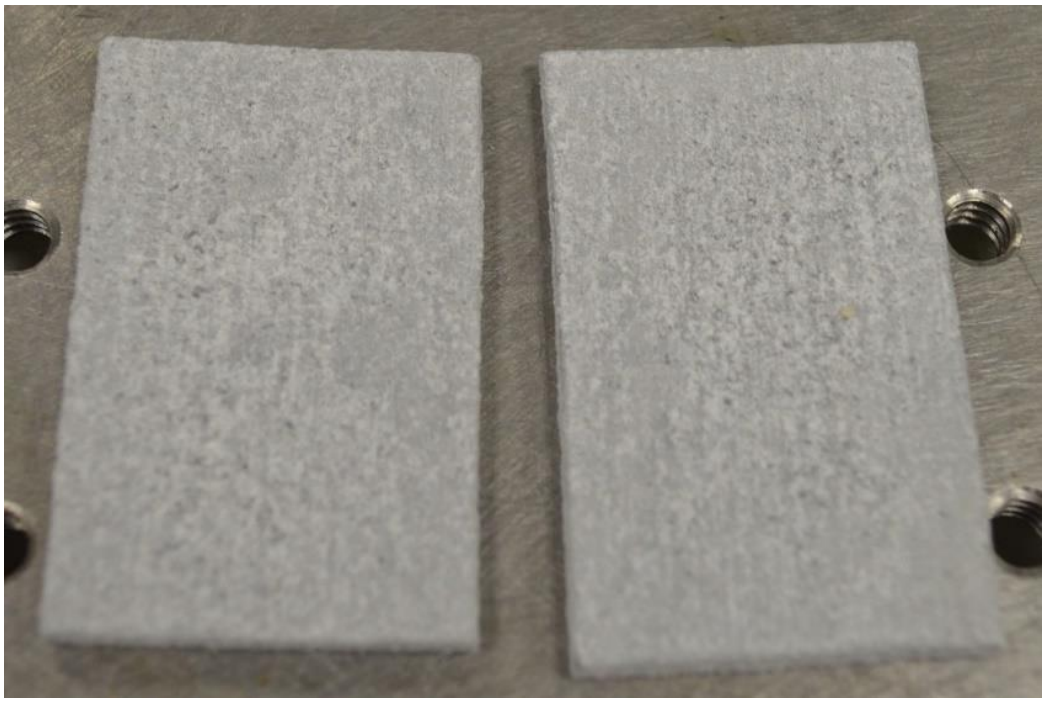

Figure A11. Etched aluminum samples after HCl immersion.

Figure A12. Teflon coated etched aluminum samples after HCl immersion.

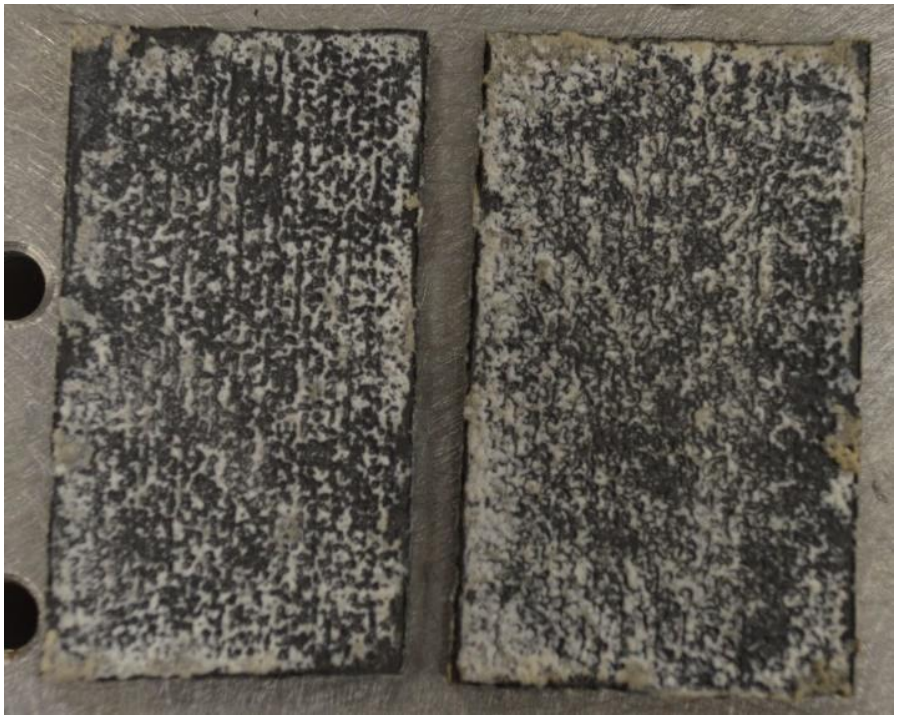

Figure A13. Etched aluminum samples after NaOH immersion.

Figure A14. Teflon coated etched aluminum samples after NaOH immersion.

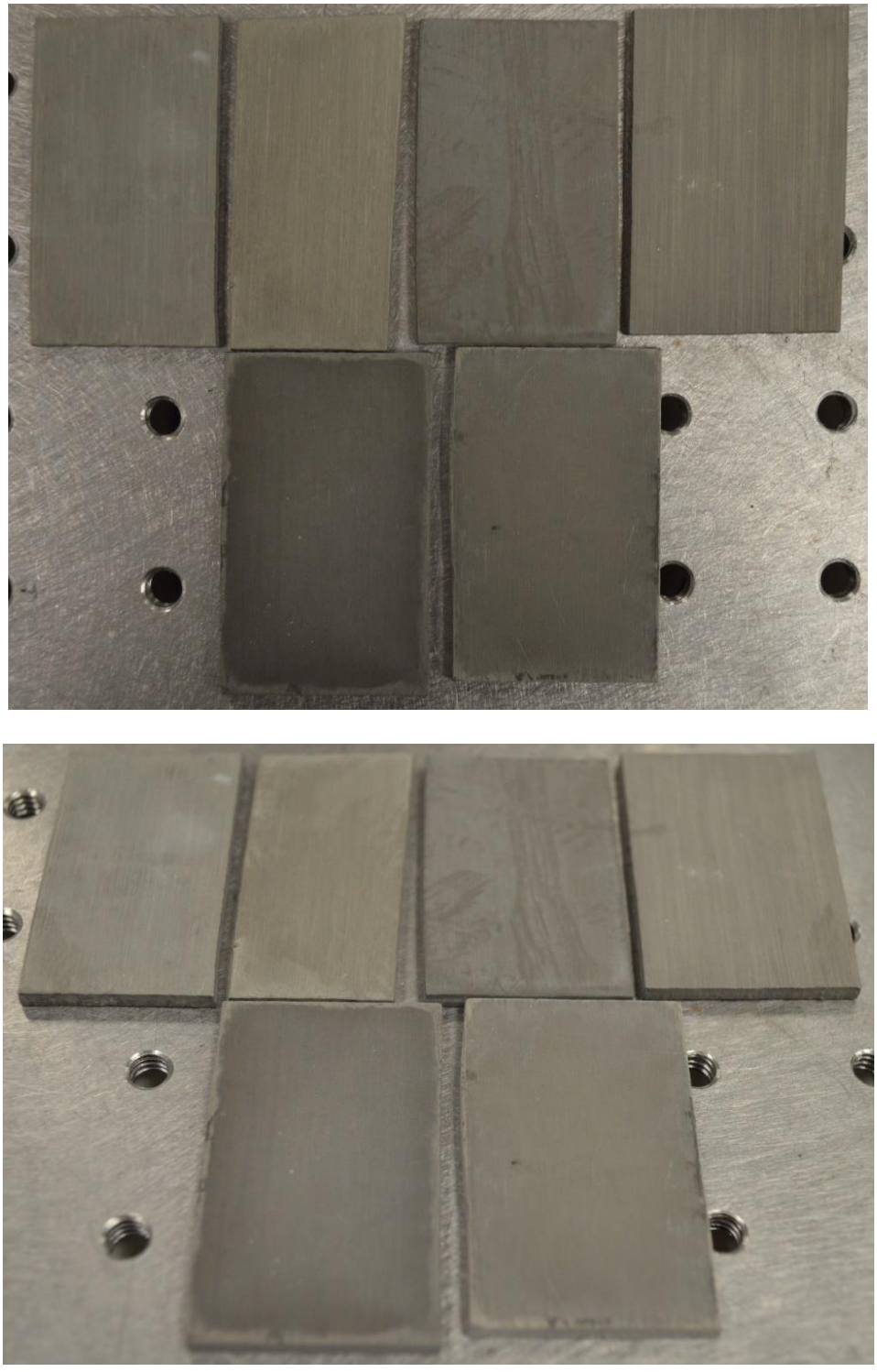

Figure A15. Etched aluminum samples after acetone immersion.

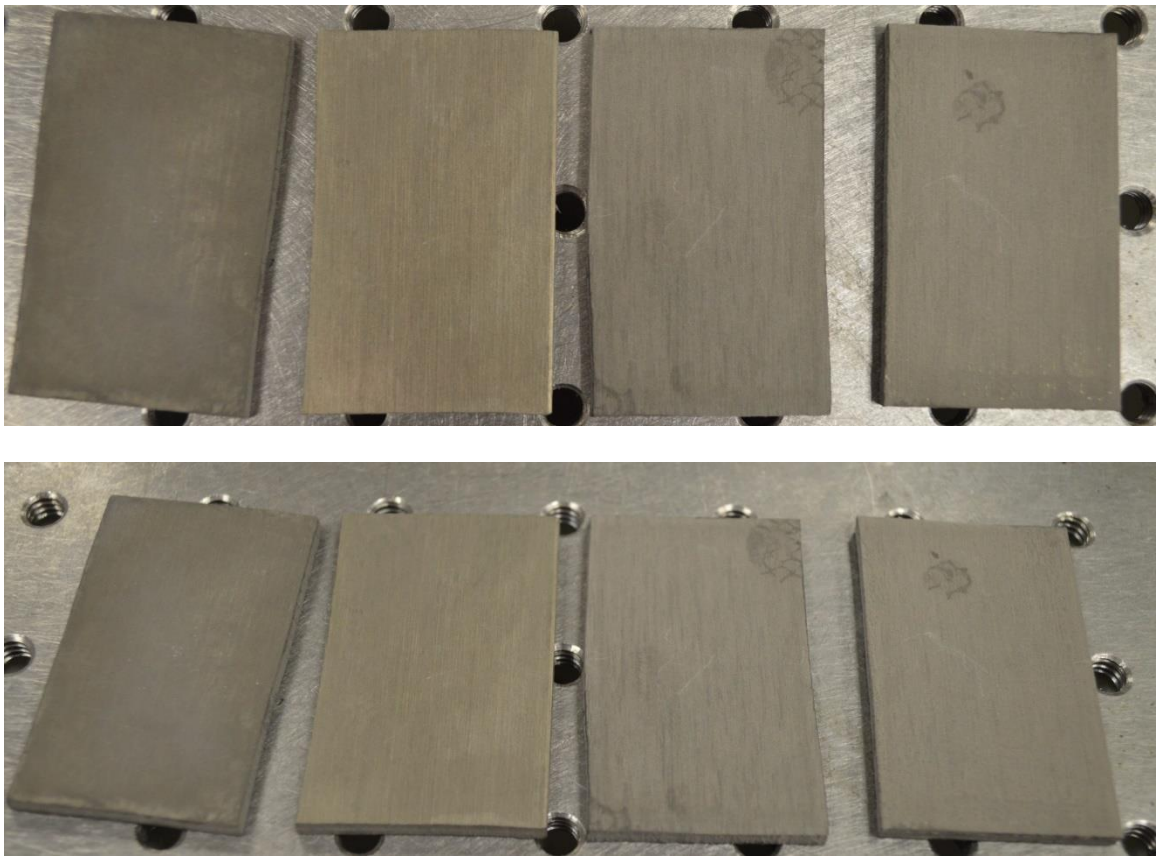

Figure A16. Teflon coated etched aluminum samples after acetone immersion.

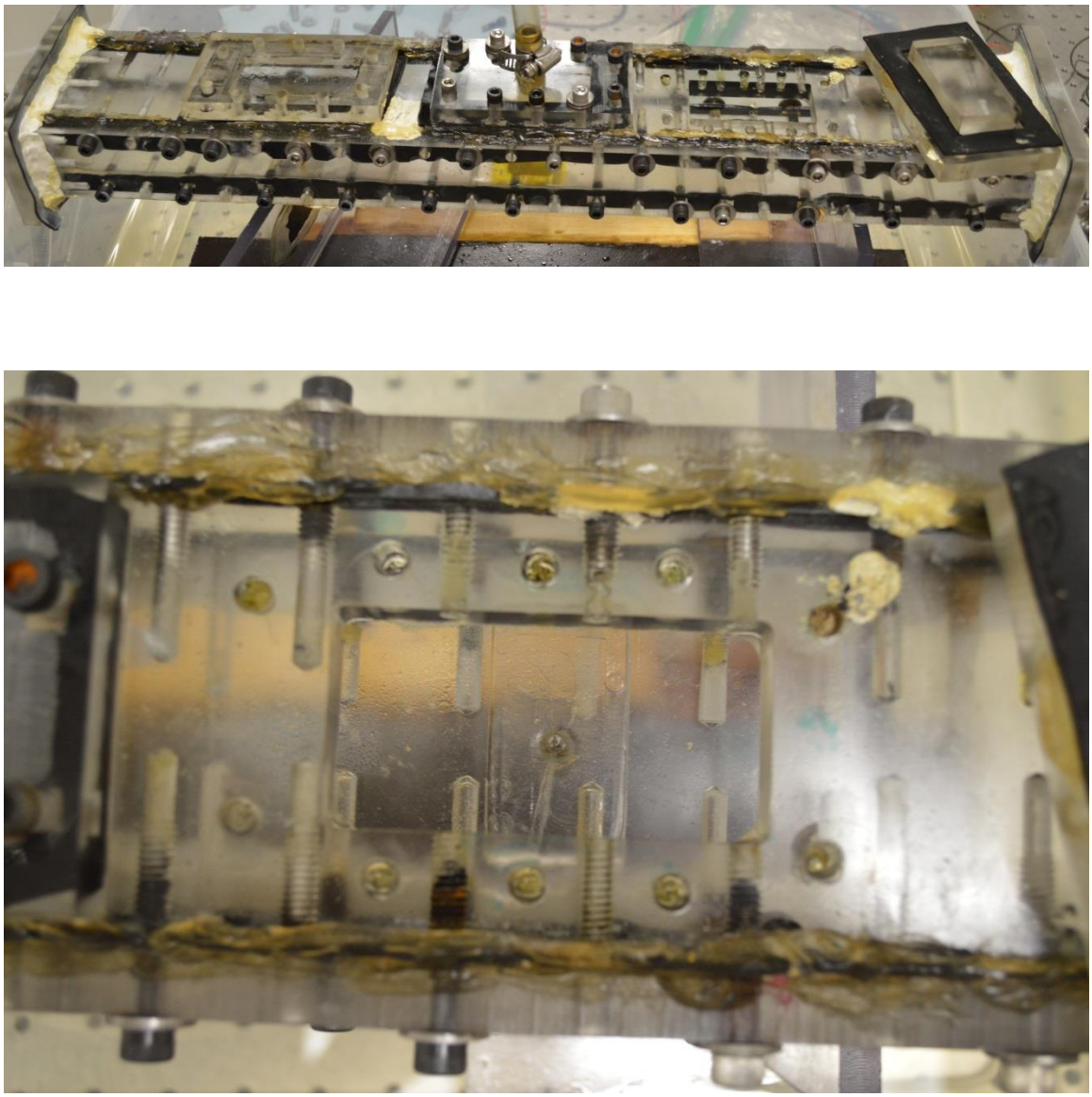

Figure A17. Custom-made test section for flow experiments.

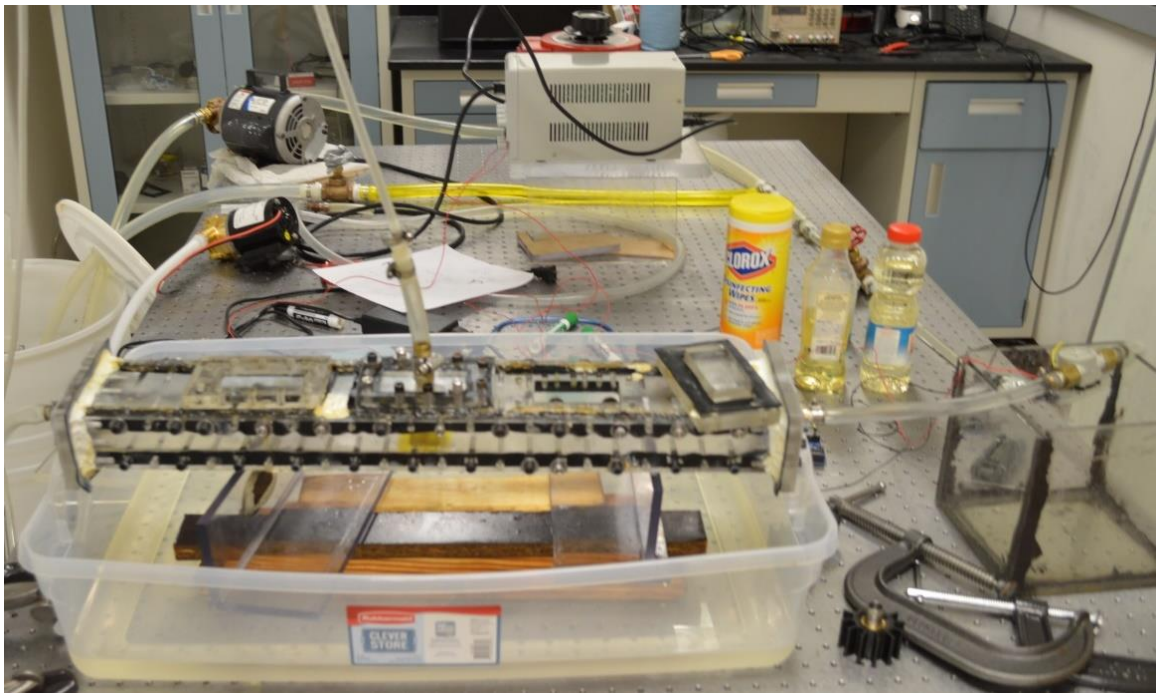

Figure A18. Experimental setup and pump for shear flow experiments.

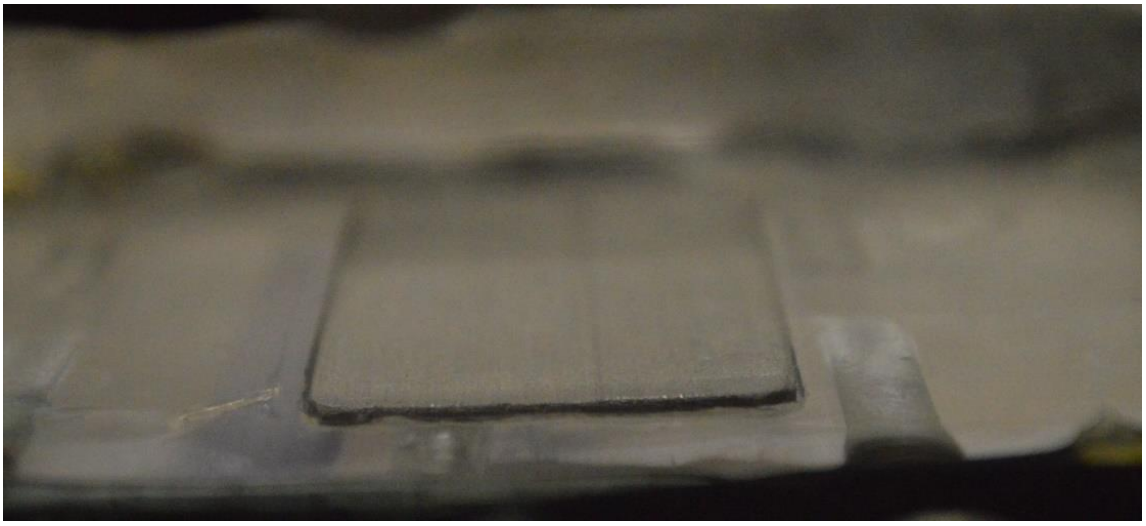

Figure A19. Oil-infused surface in test section during water shear flow experiment.

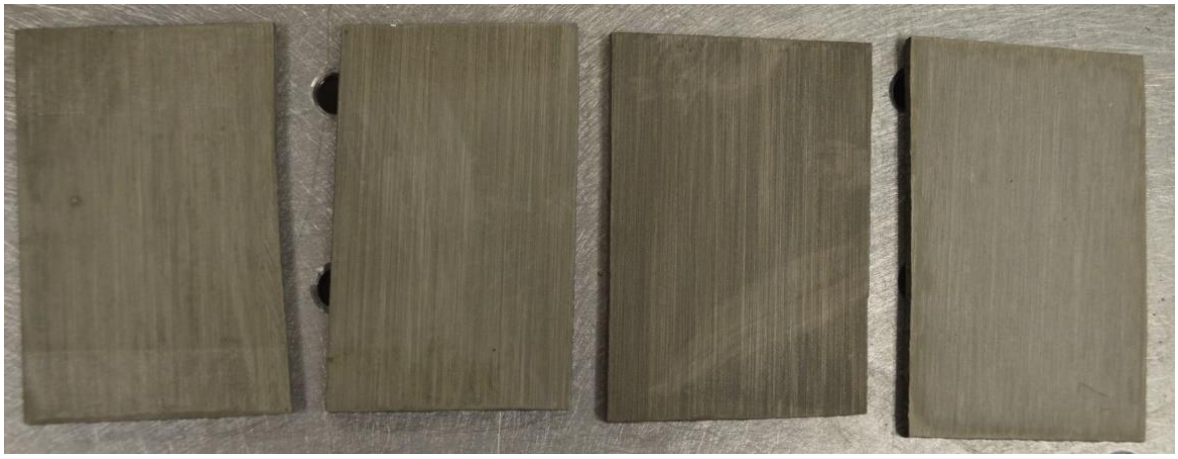

Figure A20. Oil-infused etched aluminum samples after water shear flow experiment.

Figure A21. Oil-infused Teflon coated etched aluminum samples after water shear flow experiment.

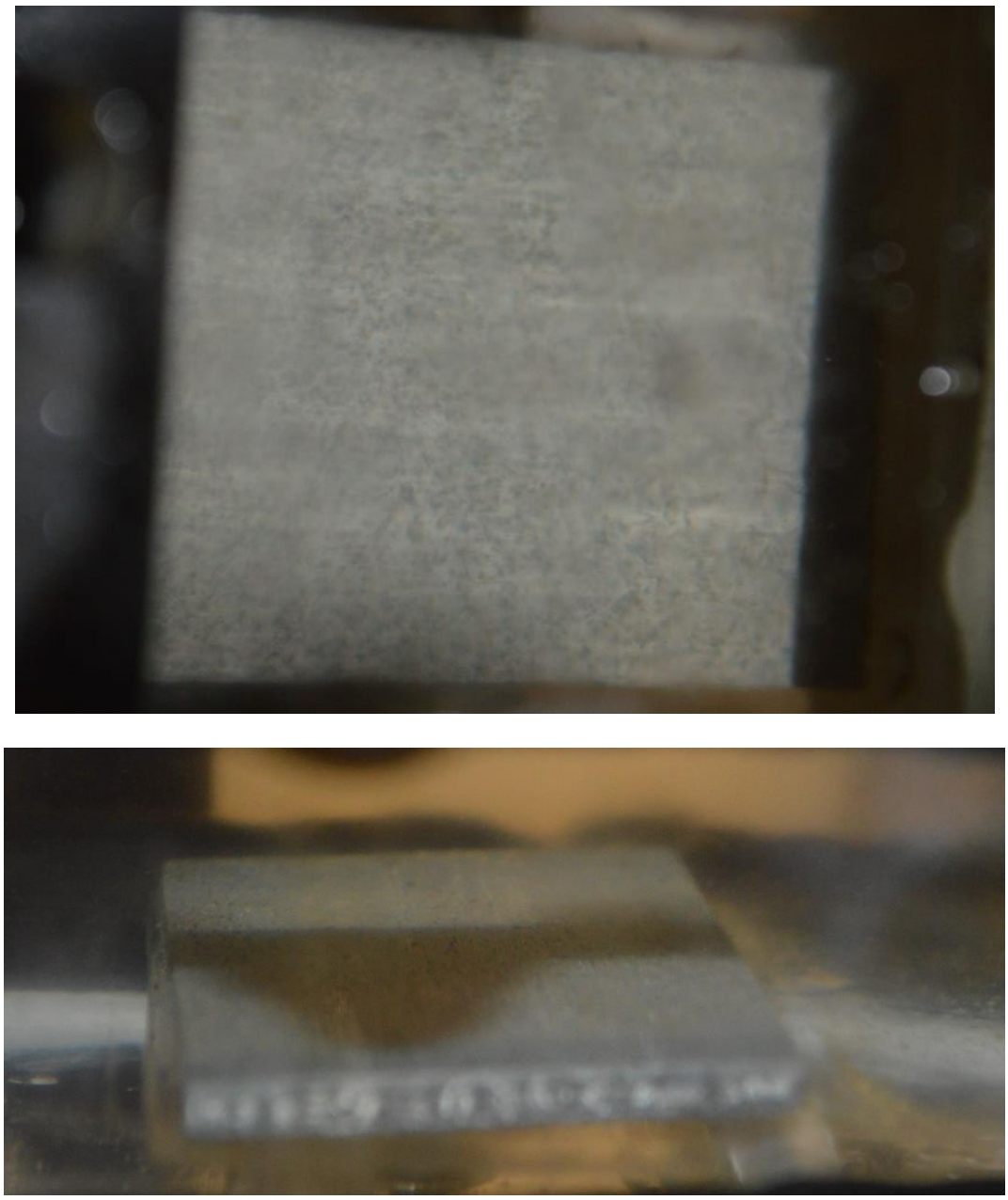

Figure A22. Water-infused sample in test section during oil flow experiment.

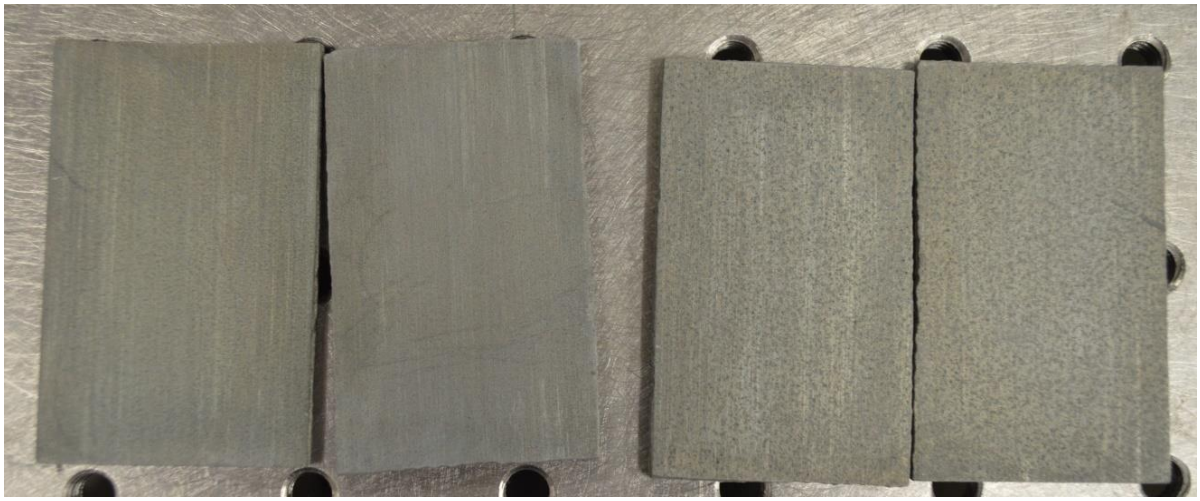

Figure A23. Water-infused etched aluminum samples after oil shear flow experiment.

Figure A24. Pressure wash setup.

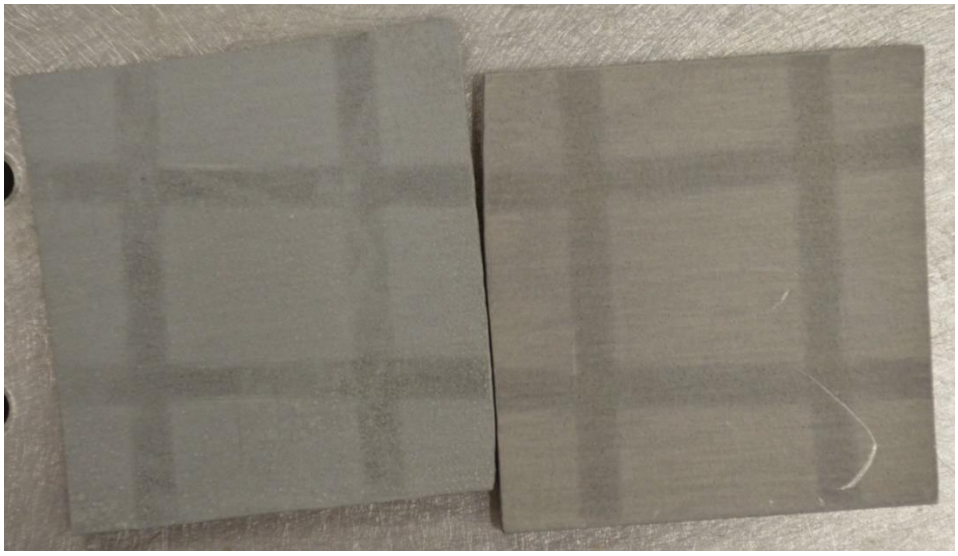

Figure A25. Surface after pressure wash test at 100 psi.

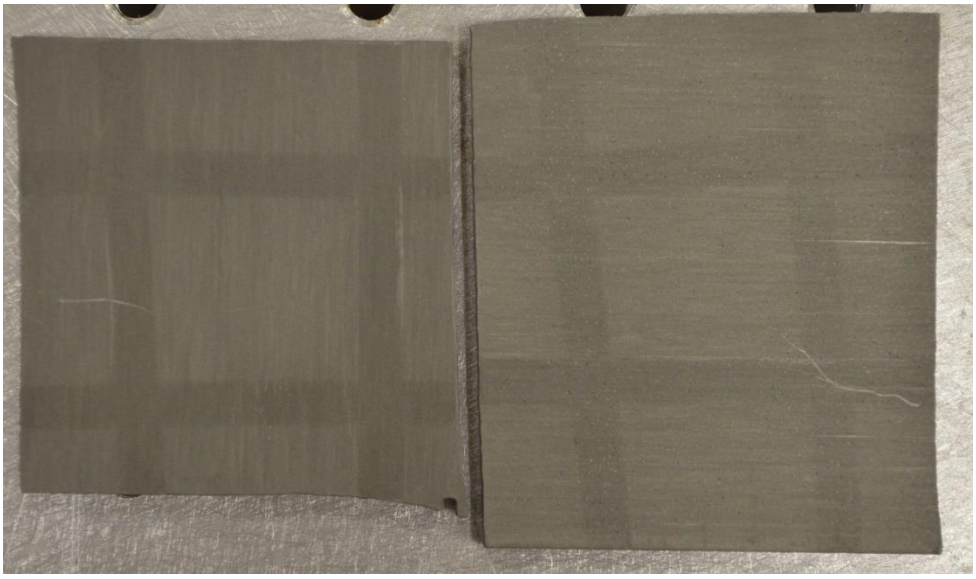

Figure A26. Surface after pressure wash test at 1000 psi.

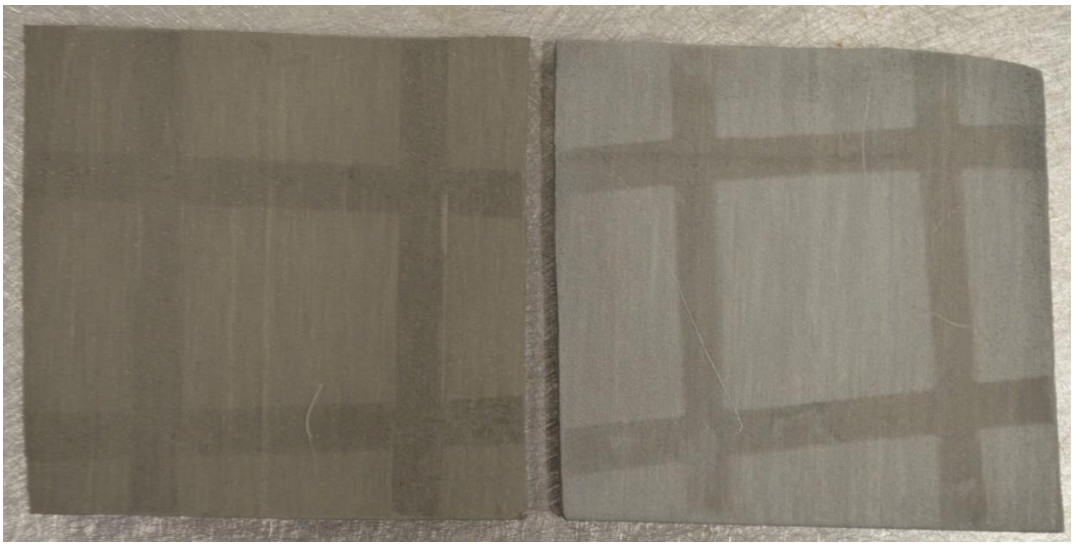

Figure A27. Surface after pressure wash test at 2000 psi.

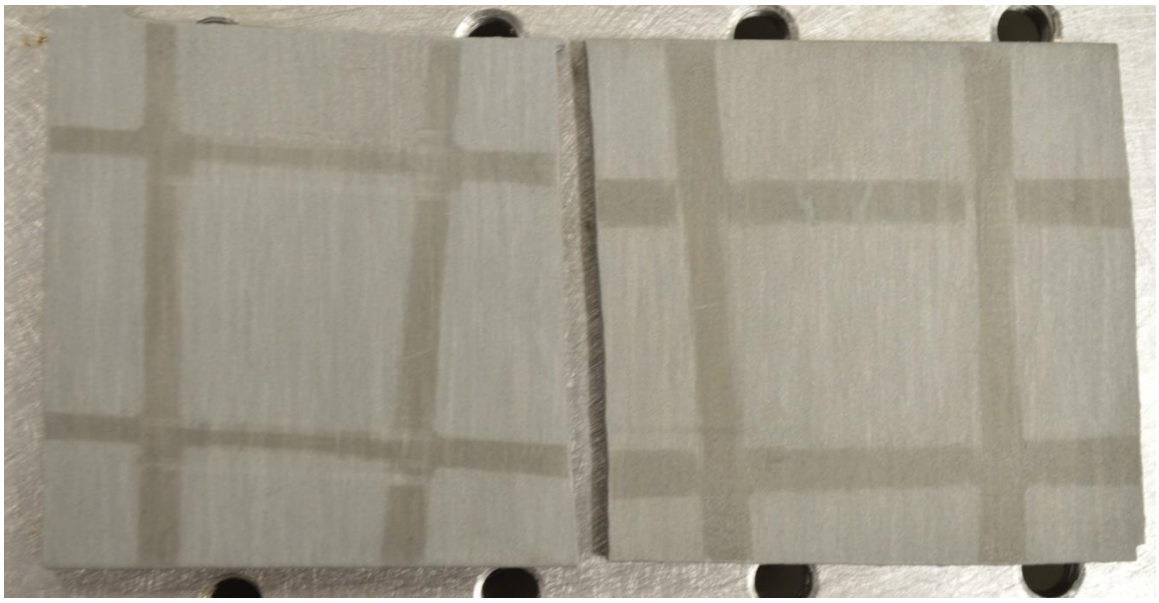

Figure A28. Surface after pressure wash test at 3000 psi.

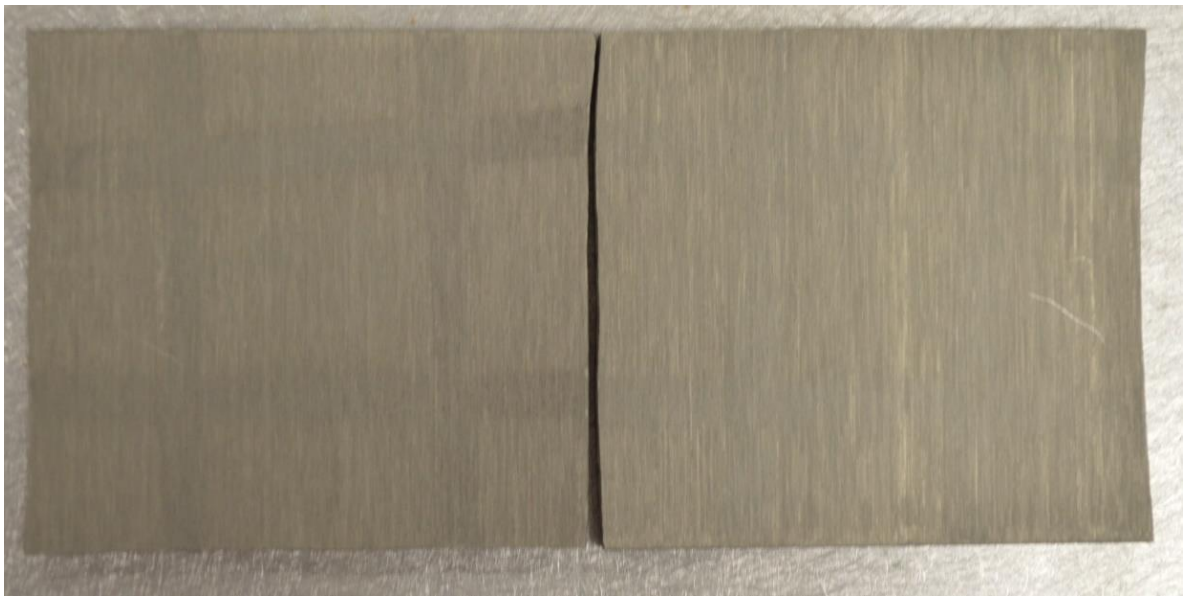

Figure A29. Surface after pressure wash test at 3400 psi.

References

1. Mugele F. and Baret J. C., Electrowetting: From basics to applications. Journal of Physics: Condensed Matter, 17, 705-774, 2005.
2. Galvin, C., Electrowetting-based Control of Water Adhesion to Surfaces. Master Thesis. The University of Texas at Austin.
3. Cai J., Nesic S. and Ward C. D., Modeling of water wetting in oil-water pipe flow, *Corrosion 2004* conference, # 04663, 2004.
4. dosSantos R. G., Mohamed R. S., Bannwart A. C. and Loh W., Contact angle measurements and wetting behavior of inner surfaces of pipelines exposed to heavy crude oil and water. Journal of Petroleum Science and Engineering, 51, 9-16, 2006.
5. Beerens J. C., Lubricated transport of heavy oil. MS thesis, Delft University of Technology, 2013.
6. Joseph D. D., Bai R., Chen K. P. and Renardy Y. Y., Core-annular flows. Annual Review of Fluid Mechanics, 29, 65-90, 1997.
7. Bannwart A. C., Modeling aspects of oil-water core-annular flows, Journal of Petroleum Science and Engineering, 32, 127-143, 2001.
8. Ghosh S., Mandal T. K., Das G. and Das P. K., Review of oil water core annular flow. Renewable and Sustainable Energy Reviews, 13, 1957-1965, 2009.
9. Bahadur, V. and Garimella, S. V., Electrowetting-based control of static droplet states on rough surfaces. *Langmuir*, 23, 4918-4924, 2007.
10. Milne, A.J.B., Amirfazli, A., Drop shedding by shear flow for hydrophilic to superhydrophobic surfaces. *Langmuir 25 (24)*, 14155–14164, 2009.
11. Cassie, A.B.D., Baxter, S., Wettability of porous surfaces. *Transactions Faraday Society 40*, 546–551, 1944.
12. Wenzel, R.N., Resistance of solid surfaces to wetting by water. *Industrial and Engineering Chemistry 28*, 988–994, 1936.
13. Zisman, W. A., "Relation of the Equilibrium Contact Angle to Liquid and Solid Constitution." (1964): n. page. *Http://pubs.acs.org*. Web. 4 Aug. 2016.
14. Panton, R. L., *Incompressible Flow*. 3rd ed. Hoboken: J. Wiley, 2005.
15. Bahadur V., Electrical actuation of liquid droplets on smooth and artificially microstructured surfaces. PhD thesis, Purdue University, 2008.
16. Ghosh A., Beaini S., Zhang B. J., Ganguly R., and Megaridis C. M., Enhancing Dropwise Condensation through Bioinspired Wettability Patterning. *Langmuir*, 30, 13103–13115, 2014.

17. http://www.engineeringtoolbox.com/liquids-densities-d_743.html

18. http://www.engineersedge.com/fluid_flow/fluid_data.htm

19. White, F. M., *Viscous Fluid Flow*. 3rd ed. McGraw-Hill Education, 2005.

20. Berker, R. A. "Intégration Des équations Du Mouvement D'un Fluide Visqueux Incompressible." *Handbuch Der Physik / Encyclopedia of Physics Strömungsmechanik II / Fluid Dynamics II,* vol. 8, pt. 2, pp. 1-384. Springer, Berlin: 1963.

21. Wu, B., A. Van Hirtum, and X. Y. Luo., "Pressure Driven Steady Flow In Constricted Channels Of Different Cross-Section Shapes." *Int. J. Appl. Mechanics International Journal of Applied Mechanics* 05.01 (2013): 1350002. Web. 4 Aug. 2016.

22. Munson, B. R., Young, D. F., Okiishi T. H., and Huebsch W. W., *Fundamentals of Fluid Mechanics*. 6th ed. Hoboken, NJ: J. Wiley & Sons, 2009.

23. Cimbala, Y. A., Çengel, J. M., *Fluid mechanics: Fundamentals and Applications.* 1st ed. Boston: McGraw-Hill Higher Education, 2006.

24. Moody, L.F., "Friction Factors for Pipe Flow," *Transactions of the ASME*, Vol. 66, 1944.

25. Colebrook, C. F., "Turbulent Flow in Pipes with Particular Reference to the Transition Between the Smooth and Rough Pipe Laws," *Journal of the Institute of Civil Engineers London*, Vol. 11, 1939.